Failure Analysis and Design Optimization of a Mill Top Journal Bearing

A final year project report

Presented to

SCHOOL OF MECHANICAL AND MANUFACTURING ENGINEERING

Department of Mechanical Engineering

NUST

ISLAMABAD, PAKISTAN

In Partial Fulfillment

of the Requirements for the Degree of

Bachelors of Mechanical Engineering

by

Muhammad Hassan Tariq

Muhammad Luqman Akhter

Taha Sharif

June 2017

EXAMIANTION COMMITTEE

We hereby recommend that the dissertation prepared under our supervision by:

Muhammad Hassan Tariq *– NUST201305031BSMME11113F*

Muhammad Luqman Akhter *– NUST201305756BSMME11113F*

Taha Sharif *– NUST201304558BSMME11113F*

Titled: **"Failure Analysis and Design Optimization of a Mill Top Journal Bearing"** be accepted in partial fulfillment of the requirements for the award of **BE Mechanical Engineering** degree.

Supervisor: **Dr Emad Uddin (Assistant Professor)**	Dated:
Committee Member: **Dr Aamir Mubashar**	Dated:
Committee Member: **Mr. Hafiz Muhammad Abdurrehman**	Dated:
Committee Member:	Dated:

_____ _____

(Head of Department) (Date)

COUNTERSIGNED

Dated: _____ _____

(Dean / Principal)

Abstract

This project is aimed at carrying out failure analysis of a journal bearing that is used to support the top roller shaft, shell and pinion of a sugar mill. The project has been performed for an industrial manufacturer of sugar mills – Qadri Group of Companies, who has had reports of multiple instances of failure of the bearing.

Failure Mode, Effects and Analysis (FMEA) has been applied to identify the root cause of the failure, with the probable causes and the standard procedure being followed as per the guidelines provided by ASM Handbook 11. After extensive testing (via multiple simulations and calculations) of the most likely causes; namely fatigue failure, operational failure, tribological failure, manufacturing faults and overheating of the bearing, the problem has been identified with the cooling system – the inefficiency of the cooling water cavity, to be more precise.

Subsequent corrective action has been taken by redesigning the cavity to be better suited for heat removal. A small scale analogous model of the part has verified that the redesigned system has a more effective heat removal ability. In fact, simulations results have revealed that the heat removal process is improved by approximately 10%. Furthermore, the mass of the material used has been reduced by about 22%, thereby reducing material costs. As a result of this project, a standard procedure of failure and design analysis of the bearing has been developed as well.

Preface

It is a great opportunity for us to have the **Bachelors of Mechanical Engineering at SMME, NUST**. In the accomplishment of degree we are submitting a project report on "Analysis of Mill Top Journal Bearing". The project is supposed to be the solution of industrial problem which was being faced by Qadri Group of Industries.

Qadri Group is the Manufacturers of Plant & Equipment for Engineering Sectors. The problem under consideration was faced in the mill top journal bearings which are manufactured by Qadri Group for sugar mills. Premature failure during the early stages of operations is a constant problem in these bearings. We stepped up to propose the solution of the problem through various analysis and developed a small scale prototype to demonstrate the improved performance of bearing.

Subject to the limitation of time, every possible attempt has been made to study the problem deeply and propose an appropriate solution. The data was acquired from industry during visit, further analyzed and interpreted and finally the results were obtained.

Acknowledgements

We are thankful to our Creator ALLAH ALMIGHTY who have guided us throughout this work at every step and every new thought that came to our mind to improve it. Indeed we could have done nothing without his priceless help and guidance.

We are also thankful to our beloved parents who were a constant source of motivation and support for us.

We would like to pay special thanks to our Supervisor Dr. Emad Uddin and Co-Supervisor Dr. Amir Mubashir for their help and guidance throughout the project.

Our thanks is extended to Mr Nouman Ali Mumtaz, out external supervisor from Qadri Group, Mr Farhan Khalid, Mr Ahmad Qadri, and other support staff from Qadri Group.

Finally we would like to thank DD MRC Col. Naveed and his whole staff who helped us in the manufacturing of prototype.

Originality Report

We hereby declare that no portion of the work of this project or report is a work of plagiarism and the workings and findings have been originally produced. The project has been done in sole partnership with Qadri Group and has not been a support project of any similar work serving towards a similar degree's requirement from any institute. Any reference used in the project has been clearly cited and we take responsibility if found otherwise.

Copyright

Contents

LIST OF TABLES

List of Figures

Abbreviations

FMEA Failure Modes and Effects Analysis

FRACAS Failure Reporting, Analysis and Correction System

FTA Failure Tree Analysis

FPM Feet per Minute

Nomenclature

D	**Diameter of the bearing**
L	Axial length of the bearing
P	Specific Steady Load
W	Load supported by the bearing
$\mathbf{h_m}$	Theoretical film thickness
c	Clearance
ε	Eccentricity ratio
$\mathbf{H_f}$	Friction power
T	Torque
ω	Shaft angular velocity
n	Speed of shaft in revolutions per second
η	Dynamic viscosity
R	Radius
h	Film thickness
A	Surface area of the bearing in contact with the shaft
$\dot{Q}$	Volume flow rate
ρ	Density of the lubricant oil
σ	Specific heat capacity of the oil
$\dot{m}$	Mass flow rate
ΔT	Change in temperature
K	Coefficient of conductivity

Δx	Thickness of bearing wall in contact with the shaft
T_2	Temperature at the inner surface of the bearing

1 Introduction

1.1 Background

The most common design configuration of sugarcane crushing mill used in Pakistan are the ones comprised of 3 and 4 roller mills. The three rollers, in both the configurations, are arranged in a triangular manner with the two bottom ones and the single top one referred to as the feed and discharge roll, and the top roll respectively, as shown in figure 1. The rollers, along with the shell

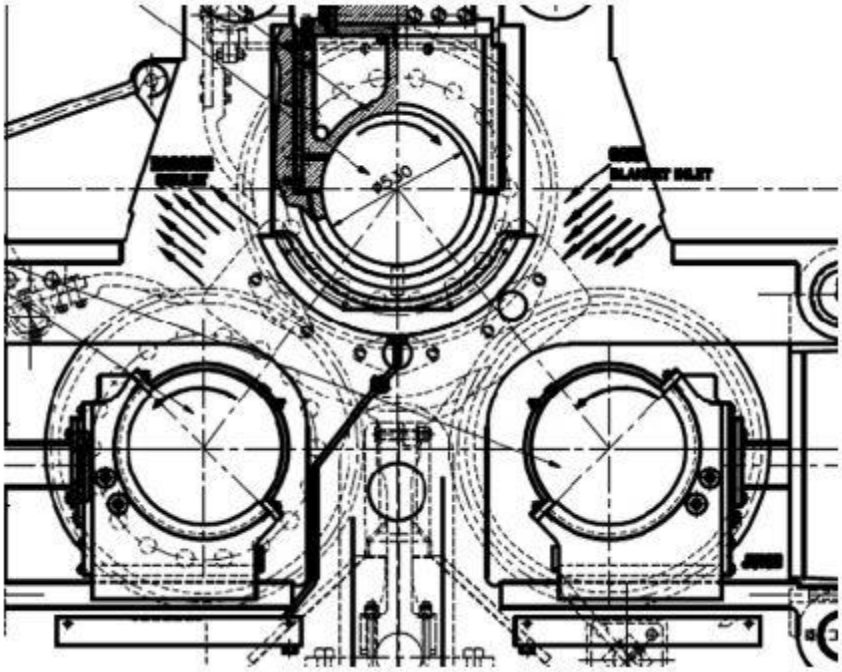

Figure 1 Cross-section of a three roll mill [1]

and pinion assembly, are supported by journal bearings.

The rotational speed of the rolls is very low (4-6 rpm) in order to maximize the extraction of juice from the cane. As the cane blanket passes through the feed and discharge rolls, the load applied for crushing is exerted by the top roller via a hydraulic transmission system with an allowance of

5-20 mm [1] for variations in thickness of the blanket. The reaction forces are supported by the top half of the top roller. An approximate load of about 20,000 kg of cane is supported by a single bearing under normal functioning. This results in significant amount of heat production and

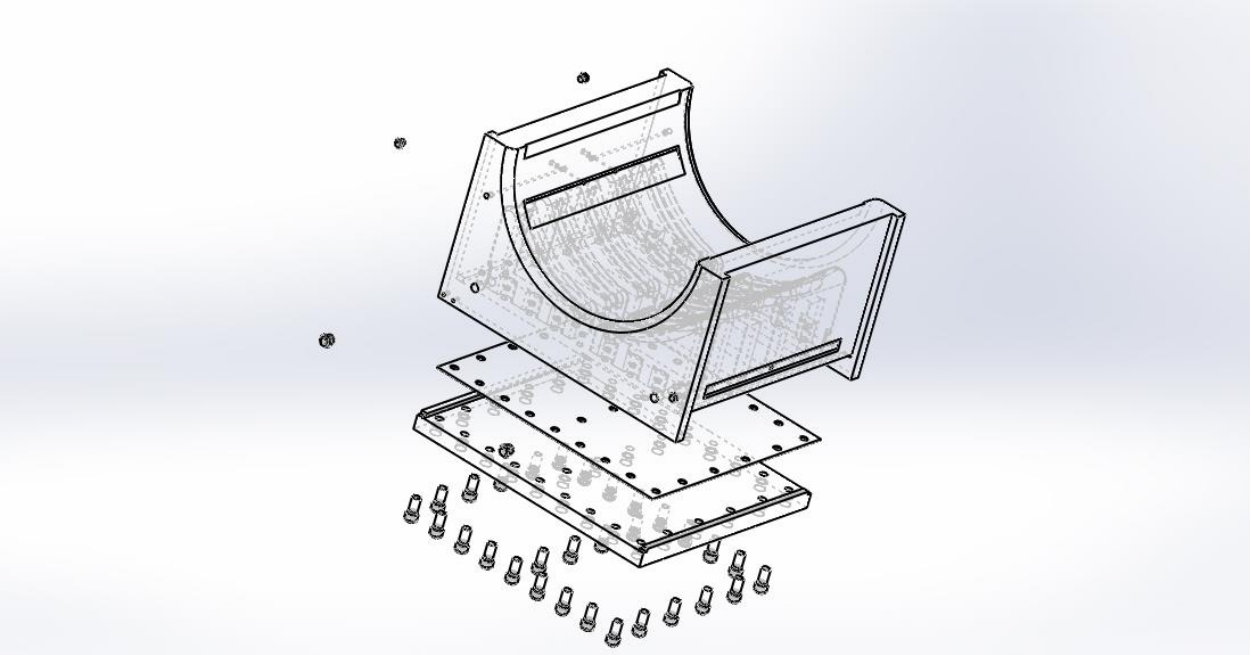

Figure 2 Exploded view of the bearing assembly

lubrication alone is insufficient for it. To cater for this, an uncommon design is followed where a cavity is made within the casing of the top half of the bearing [figure 2]. Water as a coolant runs through this cavity.

Premature failure of this bearing is a not uncommon in the Pakistani sugar industry and has been a big problem for sugar mill owners and manufacturers alike. The underlying cause for failure could be several and this project is set out to investigate the cause of failure of one such bearing, by employing a suitable failure analysis technique, and come up with subsequent recommendations to remedy the problem.

1.2 Our Project

This project was set out to carry out a detailed failure analysis of one such mill top journal bearing, for a local industrial manufacturer – Qadri Group of Companies – analyzing every potential cause using calculations and simulations, and coming up with design modification recommendations or other possible solutions.

Failure Mode and Effects Analysis (FMEA) technique was employed with guidelines extracted from ASM Handbook 11 and calculation procedures from Engineering Tribology by Gwidon W. Stachowiak. ANSYS Fluent and COMSOL were used to carry out simulations and the modelling tasks were completed in SolidWorks. Moreover, a small scale analogous prototype was to be developed to depict the proposed solution.

2 Literature Review

For the purpose of figuring out the most effective approach of failure analysis and to build up on previous research data, experiments and results, extensive studies were carried out to gain an insight to the work that had already been done in this field by reviewing the most well established methodologies, research papers by various authors on similar topics, and other available literature.

2.1 Failure Analysis Techniques

The process of collecting data and analyzing it to determine the probable causes of failures and the probability of their occurrence in a certain component under given conditions is referred to as failure analysis technique or methodology.

Among various approaches, three most widely used methods were considered before settling on Failure Modes and Effects Analysis (FMEA) technique. An overview of the three methods is given below.

2.1.1 Failure Reporting Analysis and Correction System

Failure Reporting, Analysis and Correction System (FRACAS) usually employs a software to carry out a statistical analysis and use the results to identify the most probable causes of potential failure. It makes use of the operating conditions and the instances of failure due to a certain cause to predict the mode of failure for the part under analysis. Therefore, quite obviously, is would require the data for all the previous case of failure as well. This approach was not used since the bearing under analysis was taken as a standalone case. Furthermore, the historical records of other similar components was unavailable as well, therefore, ruling out this option.

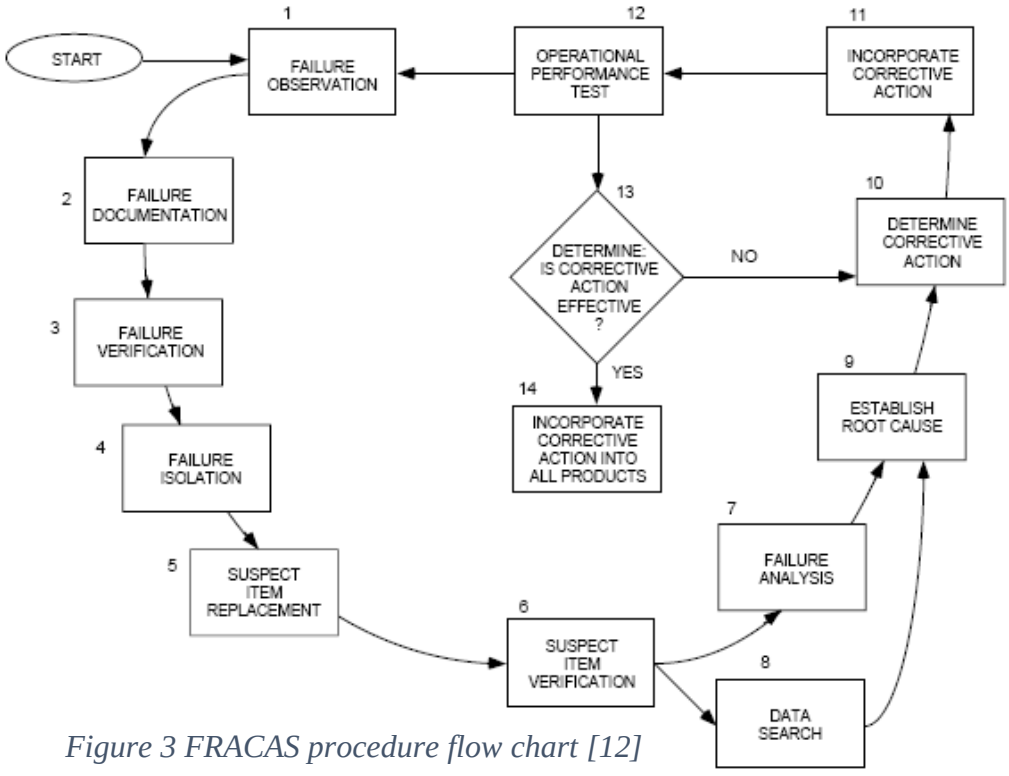

Figure 3 FRACAS procedure flow chart [12]

2.1.2 Failure Mode and Effects Analysis (FMEA)

FMEA, sometimes also called PFMEA (Potential Failure Mode and Effects Analysis) is the analytical technique that has been used to scrutinize all the potential identifiable causes and single out the reason of the failure successfully. The corresponding redesign ramification has been applied and tested for the same analysis to give decisively better results.

The procedure used by this technique involves singling out all the possible causes of failure (such as operational failure, manufacturing defect, design defect etc.) and examining each cause separately. Once the causes has been figured out, it is broken down further into subcategories, if applicable, to cater for the exact problem.

For this project, a slight modification has been made to the conventional FMEA process. The severity of a certain cause, and the risk priority numbers (RPN) have not been accounted for, as each cause has been distinctly categorized as possible or not possible.

2.1.3 Fault Tree Analysis

Fault tree analysis (FTA), developed by Bell Laboratories, is another popular analysis technique that was considered. It is very similar to FMEA in its approach. However, it differs in certain fronts that lead to the dismissal of its application.

FTA uses a graphical method using Boolean functions to form a hierarchical progression of potential causes leading to failure. The potential hazard is identified and corrected upon after evaluation of all the branches. FTA, however, is not just limited to hardware failure modes. It includes software failure, system failure, and human failures alongside as well, and their combinations. Since the scope of our project was limited to mechanical causes of failure, FTA was deemed unsuitable for this case.

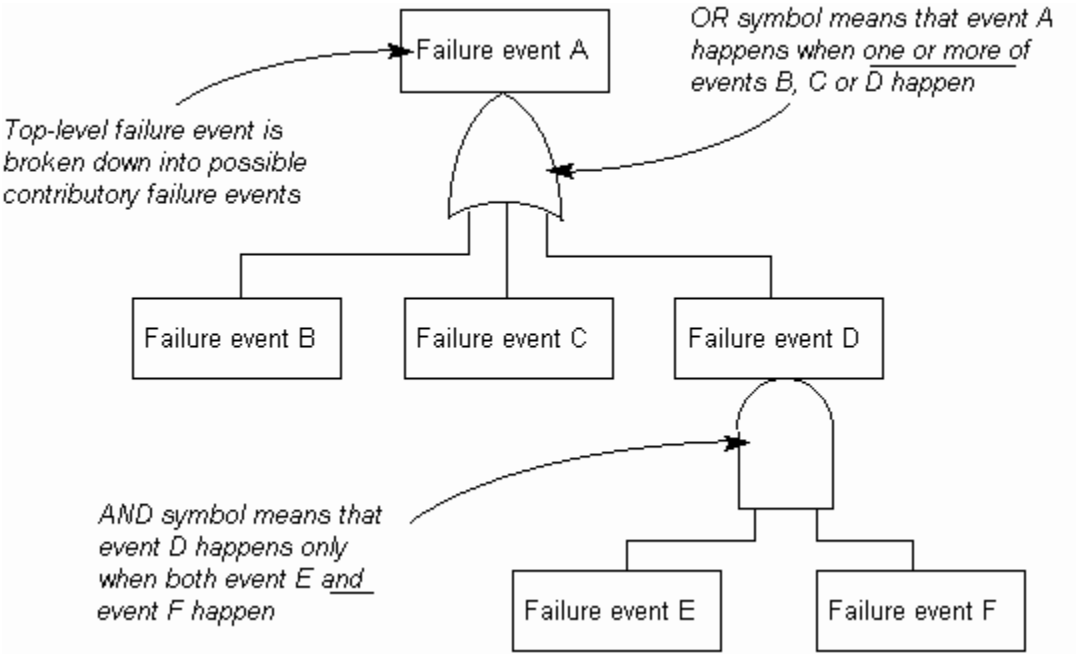

Figure 4 FTA Procedure [11]

2.2 Operating Conditions

The operating conditions, as recommended by the manufacturer, are provided in the Table 1 below. For the purpose of this study, it has been assumed that the conditions were maintained in the proposed operational limits.

It is to be noted that these conditions are dictated by the manufacturing material which is a type of bronze (Cu-85%, Sn-6%, Zn-5%, Pb-4%). In some studies regarding the sugar mill journal bearing, this Cu-Sn bronze has been referred to as brass as well.

Parameter	***Condition***
Speed	4-6 RPM
Loading	20 Ton
Type of Coolant	Water
Coolant Inlet Conditions	25°C and 3 bar pressure
Coolant Flow Rate	24 L/min
Type of Lubricant	Castrol SMR Medium Oil
Lubricant Flow Rate	~ 115 Gallons/hour
Material Limiting Temperature	~ 55-60°C

Table 1 Operating Conditions

The properties of oil as provided by Castrol are as shown in the table below.

Name	***Methods***	***Units***	***Alpha SMR Medium***
Color	ASTM D1500	-	Black
Density @ 20°C	ISO 12185 / ASTM D4052	Kg/m^3	949
Kinematic Viscosity @ 40°C	ISO 3104 / ASTM D445	mm^2/s	12005
Kinematic Viscosity @ 100°C	ISO 3104 / ASTM D445	mm^2/s	50.5

Viscosity Index	ISO 2909 / ASTM D2270	-	84
Pour Point	ISO 3016 / ASTM D97	°C	0
Flash Point – open cup method	ISO 2592 / ASTM D92	°C	250
Bitumen	-	-	Yes
Compounding	-	-	Yes
EP Additives	-	-	Yes

Table 2 [2] Lubricant Properties

2.3 Design Parameters

The research and experimentation of D. J. Hargreaves, Malcolm E. Leader and S. M. Muzakkir has worked out the feasibility of these operating conditions by studying and formulating the behavior and effects of certain design parameters. These parameters have been tested for the bearing under the conditions recommended by Qadri Group.

2.3.1 Specific Steady Load

Specific steady load determines the stability and the heat generation for the bearing. Leader, in [3], says that an extremely light loading results in significant oil whirl and can cause problems related to instability. Whereas, a very heavily loaded bearing would result in a large amount of friction and, hence, heat generation. The loadings are classifies by Hargreaves as in the following table.

Specific Steady Load (PSI)	***Classification***
0-50	Very Light
50-100	Light

100-200	Moderate
200-300	Heavy
>300	Special Design

Table 3 [3] Specific Steady Load Classification

The bearing under consideration has a specific steady load of 47.86 PSI which signifies that heat generation is within reasonable operational limits. Since the speed of the shaft is very low, the problems associated with oil whirl and instability are ruled out.

2.3.2 Surface Speed

Surface speed, as the name suggests, is the speed of the outer most rotating surface at a given rpm and is calculated in feet per minute (FPM). The higher the rpm, the higher the fpm. Leader suggests in [3] that a higher surface speed can result in turbulence of the oil film and, ultimately, ineffective lubrication and higher heat generation due to increased friction. Generally, speeds lower than 1500 FPM are considered safe for most turbomachinery. Since the surface speed for this bearing is just 34 FPM (which is to be expected given an rpm of 5), chances of turbulence in oil film are close to being nonexistent.

2.3.3 Material Limitations

H. M. Muzakkir in [1] says that the limiting pressure of a bronze bearing, of composition used in sugar mill journal bearings, is 50 MPa. The yield strength of bronze bearing is approximately 20 MPa. The loadings, as a standard practice in sugar mills; particularly in the subcontinent region, are 10 MPa. This is well under the limiting values and should not cause any issues that might result in failure of the component.

2.4 Lubrication Regime

The development of oil film as the rotation of the shaft starts and its maintenance during its continued operation is a very key factor of bearing safety. The type of oil film that develops as a result of shaft motion determines the effectiveness of lubrication. In [4], Sumit Singhal has defined three regimes of lubrications.

- *Boundary Lubrication:* Boundary lubrication can potentially be the most damaging lubrication phenomenon. This occurs when the two surfaces directly in contact with each other due to a nearly nonexistent lubricant film between them. The resultant metal to metal contact can cause immense wear of the components with prolonged usage.
- *Mixed Boundary-Hydrodynamic Regime:* This is an intermediate condition between boundary lubrication and fully developed oil film. The partial layer can allow the accumulation of contaminants and can result in failure as well.
- *Hydrodynamic Regime:* This regime is achieved when the layer has fully developed and there is no metal to metal contact and, hence, no friction due to this. Therefore, chances of wear of the bearing are also minimized.

D. J. Hargreaves and S. M. Muzakkir in [5] and [1] respectively have conducted experiments and studies to figure out the lubrication regime that is attained in sugar mill bearings. Hargreaves has made use of the E.S.D.U calculation method of 1966 and has further employed a computer program which was developed to verify the results and further extend them to a more realistic model of the bearing under testing. He has proposed the nature of the lubrication to be boundary.

S. M. Muzakkir carried out an extensive investigation with the first part of the research involving rigorous calculations starting off from Reynold's Equation. A test rig was setup to confirm the

results for the bearing by running it under the standard conditions and the same conclusion was reached as Hargreaves with Muzakkir suggesting only a slight chance of fixed boundary condition's development.

The theory is indicating a fair probability of lubrication being a prime factor in failure, and this has been tested for later in this analysis.

3 Methodology

The findings gathered from the literature review and the data provided by Qadri Group have been combined with the guidelines of failure analysis provided by ASM Handbook Vol 11 – Failure Analysis and Prevention. The inspection procedure has been followed as closely as possible, keeping in view the scope of the project, by visiting the manufacturing facility of Qadri Group and observing the failed specimen. The bearing has been observed in its functional state as well at Ramzan Sugar Mills.

Furthermore, multiple simulations have been carried out in ANSYS Fluent and Comsol to test for the heat transfer and oil film development processes. The results have been attempted to be verified via calculations as provided by Malcom E. Leader in [3] and by engineering tribology.

An analogous scaled-down model prototype has been developed to depict the improvements in the original design and the recommended design, once the problem has been identified and catered for.

The work break down structure of the process is shown in the WBS figure below.

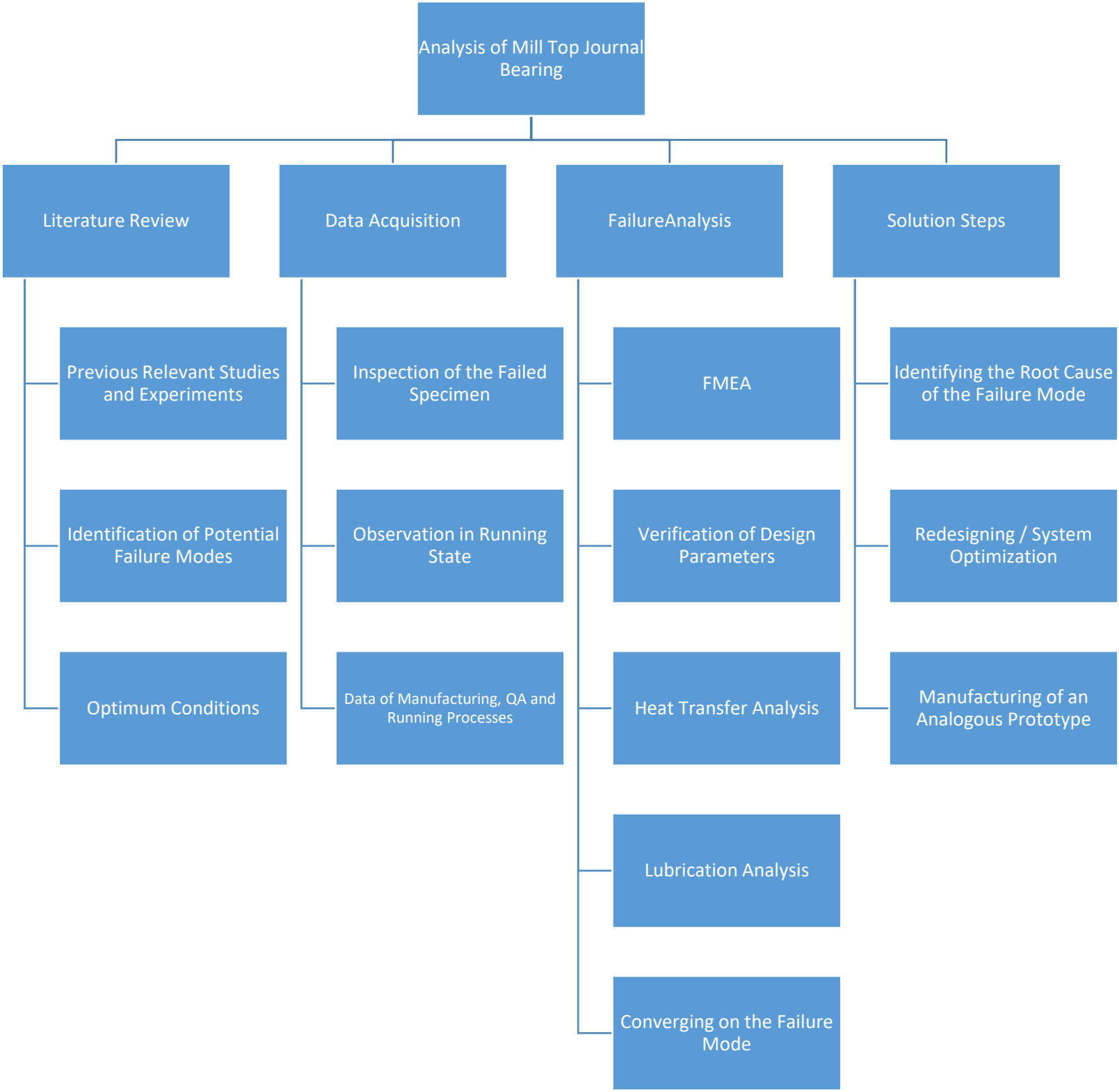

Figure 5 WBS of the analysis

The process was followed as depicted in the summarized flow chart.

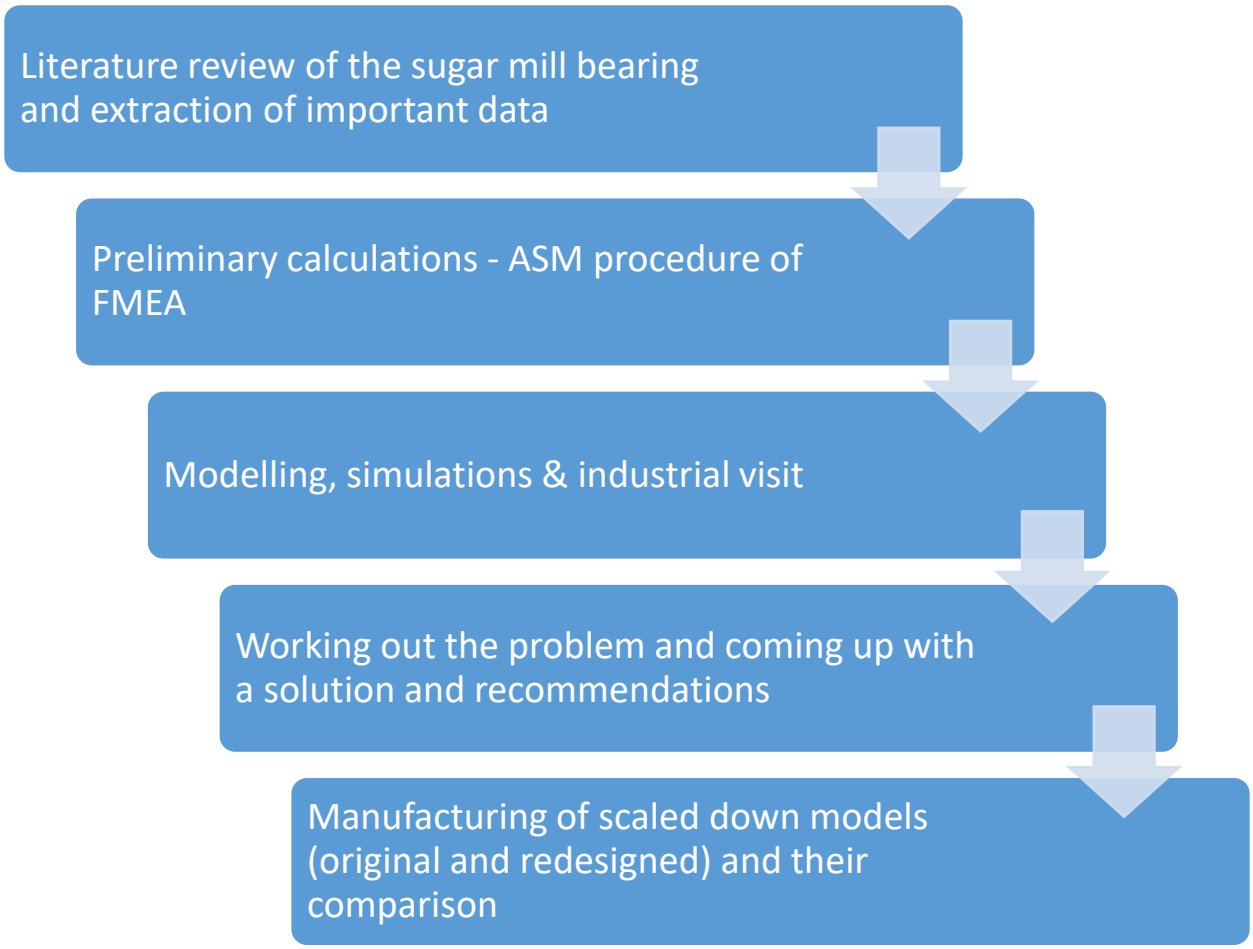

Figure 6 Flow chart of the analysis

4 Data Acquisition

4.1 ASM Procedure for Analysis [6]

The following guidelines were used as closely as possible to acquire as much of the data available from the failed specimen.

- Do not clean the machine or bearing before the first examination.
- Obtain a history of operation of the bearing, lubricants used, other failures in the system, and histories of bearings in similar machines. It is often helpful to

get comments on machine behavior from technicians and mechanics instead of from engineers and managers

- Examine the bearing in its normal operating position, and look for evidence of abnormal environment and surrounding hearing and damage. Photograph the machine, both close up and overall
- Examine all parts, wear debris, decomposed lubricant, and so on, during disassembly. Retain samples of debris and lubricant, and retain both halves of a sliding pair
- Use a low-power (binocular, if possible) optical microscope for observing the uncleaned parts, and try to establish the progression of damage☒
- Use a higher-power optical microscope if something interesting appears and it is not yet appropriate to clean the parts thoroughly☒
- If the parts can be cleaned, it is usually most convenient to use the scanning electron microscope, even for magnifications down to 20 ×, because the greater depth of field of the scanning electron microscope is far less likely to obscure details on a rough surface than an optical microscope at the same magnification☒
- X-ray microanalysis is a convenient tool for detecting material transfer, the composition of embedded particles, and loss of layers of multilayer bearings☒
- Look for evidence of fretting, poor bonding between layers in the bearing, oxidation, plastic flow, fatigue, high temperature, scuffing, and embedded particles (often found in regions of low pressure in the bearing)
- Analyze the lubricant for debris particles and by spectrographic methods to measure the concentration of dissolved elements, and compare the results with a normal lubricant. The lubricant supplier may have access to the characteristics of such normal lubricant. Determine the possible sources of high amounts of dissolved elements☒

☒ = step skipped

4.2 Visual Inspection and interpretation

Following conclusions can be drawn from the visual inspection of the defected bearing:

- As the bearing failed in early durations of operation, which is also called premature failure, we can negate the factor of fatigue failure.
- We know that for hydrostatic lubrication conditions, specific film thickness $\lambda<1$. This tells us that there always will be wear under hydrostatic conditions.
- Long axial cracks can be seen running through the surface of the bearing.
- Also there seems to have occurred fair amount of wiping on the bearing surface that shows excessive load and high temperature of oil. Discoloration is also present at certain locations which proves that temperature in the bearing exceeds the limits. These prove to be the main reasons of the premature failure in the bearing.
- In the failed bearing, it can be seen that the material has worn down in the direction of motion and deposited somewhere else. Tis also shows the presence of high temperatures during operation.
- In this bearing, an axial groove is given which helps in distributing the lubricant in bearing and increases the load bearing capacity. The experimental study by S. M. Muzakkir, Hirani & Thakre regarding the effects on wear of different grooves in heavily loaded, slow speed journal

Figure 7 Failed specimen I

bearing in [7] showed that only giving an axial groove is not preferable. The results of the study show that an axial groove alone causes a lot of wear. So it is advised to use both grooves together. In our case, this could also prove to be one of the reasons for wear.

Figure 9 Failed specimen II

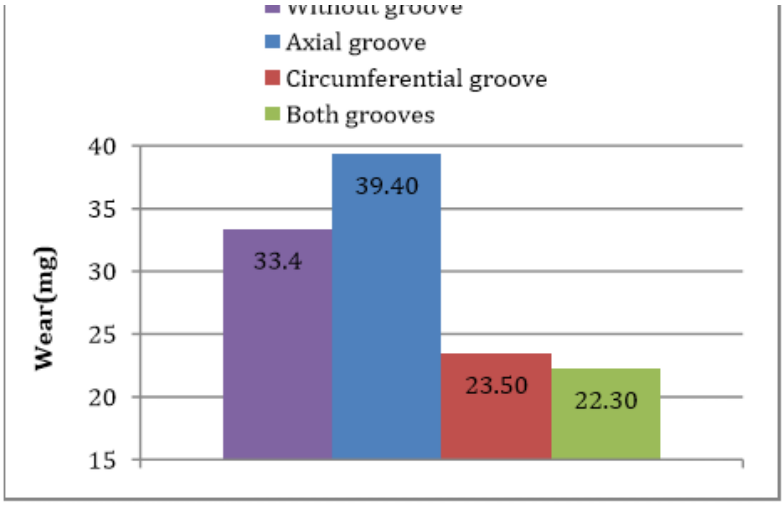

Figure 8 Wear vs Groove type [7]

4.3 Temperature Measurement of Prototype

A k-type thermocouple was used measure temperature of the coolant water at regular intervals and maintain a constant check. The program code is provided in appendix 3.

5 Lubrication Analysis

The main aim of lubrication analysis was to determine whether the film thickness was sufficient or not and also to check whether the bearing failure was occurring due to insufficient lubrication as listed in FMEA Analysis as one of the possible modes of failure. This analysis included modeling thin film on any of the commercial software and then check its behavior according to our own bearing parameters.

5.1 ANSYS

We started our analysis on ANSYS Fluent. The geometry used is shown below

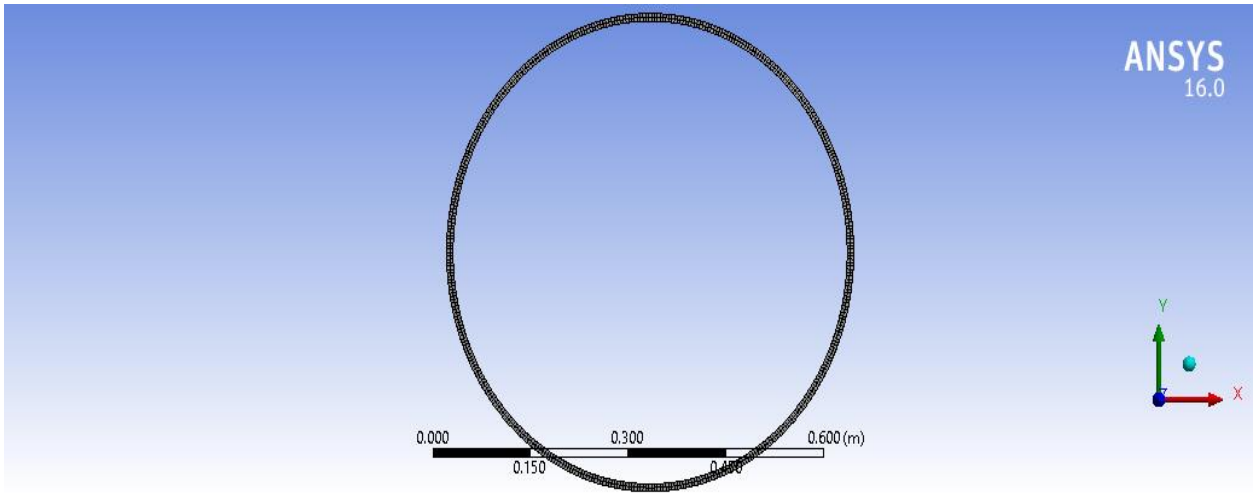

Figure 10 Geometry and mesh - ANSYS

Magnified view is shown below

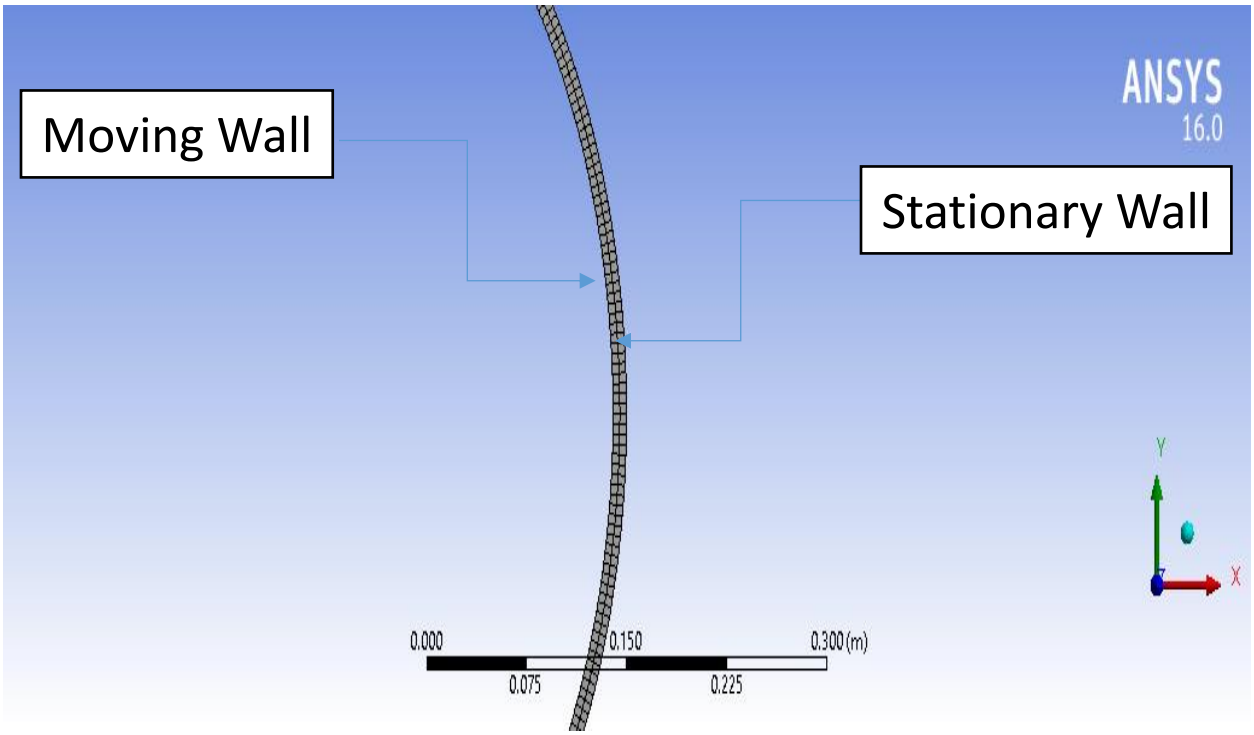

Figure 11 Zoomed section of Fig 10

Two edges can be seen in the geometry with mesh present between them. Outer edge is stationary (Bearing surface) while inner edge (Journal shaft) is rotating at 5 rpm. In between these two edges there is a thin layer of lubricant (Castrol SMR Medium) whose properties have been used in the analysis. Simple energy equation was solved. In the post processing stage we wanted to have wall fluxes so that we can use those values of flux in our heat transfer analysis. We also wanted to have some means to plot film thickness throughout the rotation of journal. We gave outer wall temperature at the outer wall to be 45 degrees.

5.1.1 Post Processing

Following were the results obtained in post processing.

- *Velocity Contours*

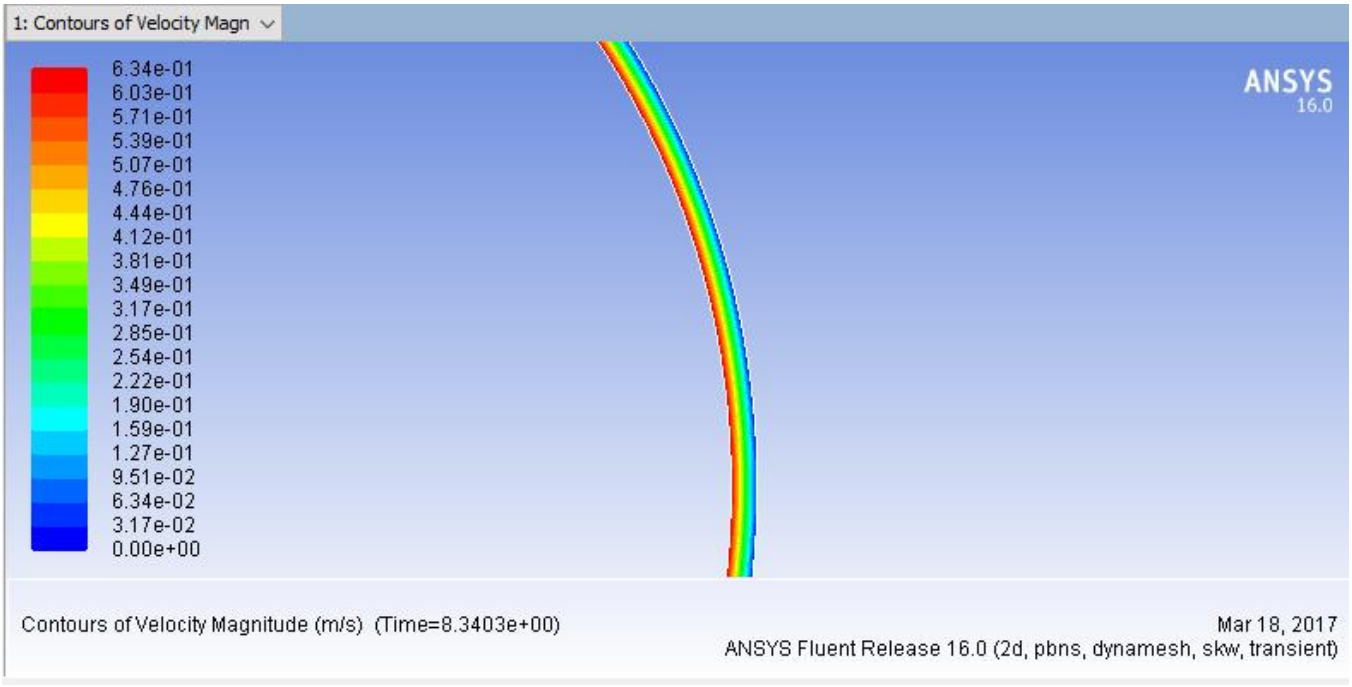

Figure 12 Velocity contour

It can be seen that the fluid near the rotating wall is also rotating at a speed nearly similar to journal speed while the fluid near to stationary wall was also stationary.

- *Temperature and Wall Fluxes Plot*

Temperature and wall flux plots are shown below. The maximum value of total surface heat flux came out to be 0.193 W/m^2. This value is highly unrealistic because theoretically calculated value of flux was approximately 1000 W/m^2.

From temperature plot we can see that temperature is constant throughout the thickness of lubrication which is also unrealistic. So we can conclude that this analysis is insufficient to provide us realistic results. The reasons for such results are discussed in the next section.

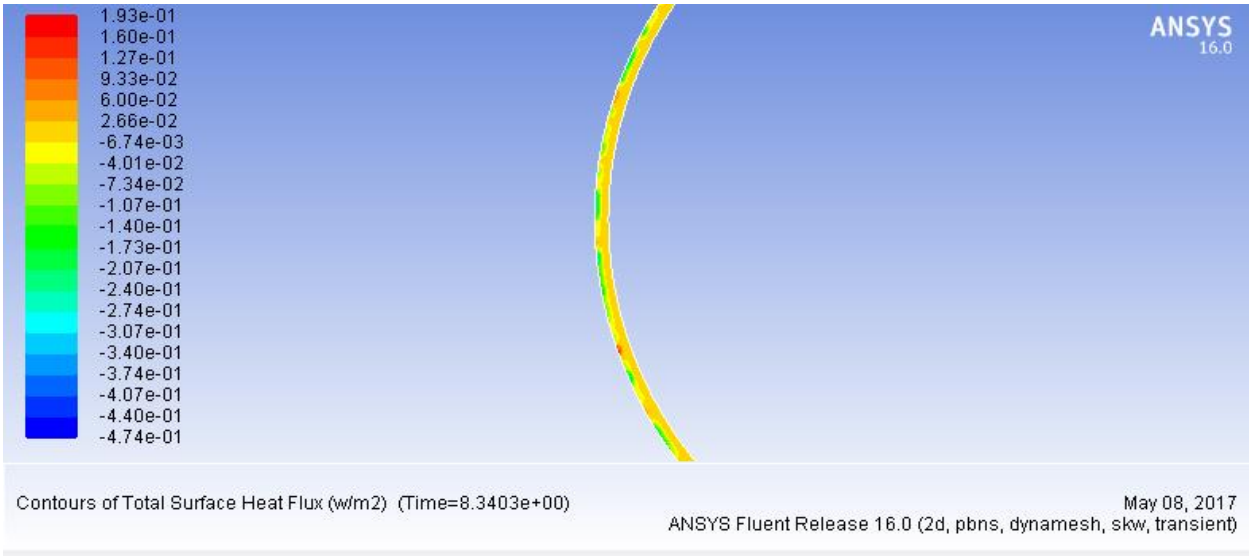

Figure 14 Total surface heat flux plot

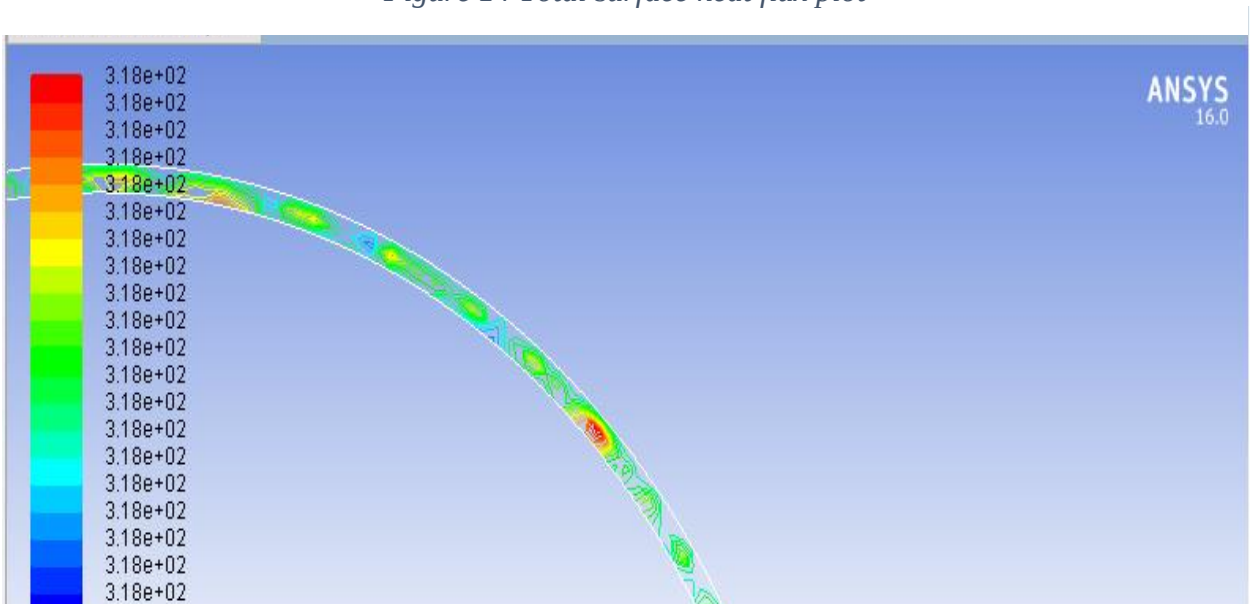

Figure 13 Temperature plot

5.1.2 Limitations of Thin Film Flow in ANSYS

In thin film flow analysis the behavior of fluid changes significantly so we cannot model thin film as easily as we model other simple phenomenon In ANSYS Fluent. Also ANSYS don't have any

in built thin film flow analysis module. In our case we wanted to have film thickness plots from where we could extract minimum film thickness location and maximum pressure created by this film on bearing surface. ANSYS didn't have any such tool so we shifted our analysis to some other commercial software and we chose COMSOL Multiphysics.

5.2 Comsol

Comsol Multiphysics has a built in "Thin film flow physics module for hydrodynamic journal bearings". We used this module and modified it for our case by using values of various parameters i.e. diameters, eccentricity, diametric clearance etc. What this module does is to prompt us to enter the values of the parameters and then gives us results in the form of various plots i.e. velocity vector plot, pressure plot and film thickness plot. These plots are very helpful to deduce the conclusions regarding lubrication sufficiency.

Geometry used is shown below. It is the surface of journal upon which various plots and results will be displayed.

Flow physics and boundary conditions are given below

- Thin Film flow module was used
- Governing equation is the Reynolds equation which is being solved here for pressure, velocity and film thickness as a function of diametric clearance
- The pressure at the ends of the cylindrical journal is assumed to be similar to the ambient pressure. Therefore, the border conditions are

$$p = 0 \quad at\ z = 0, L$$

Where L is the length of the cylindrical journal.

- Nominal clearance c and eccentricity ratio ε are known quantities.

Eccentricity ratio for sugar mill bearing is around 0.9 because of larger loads.

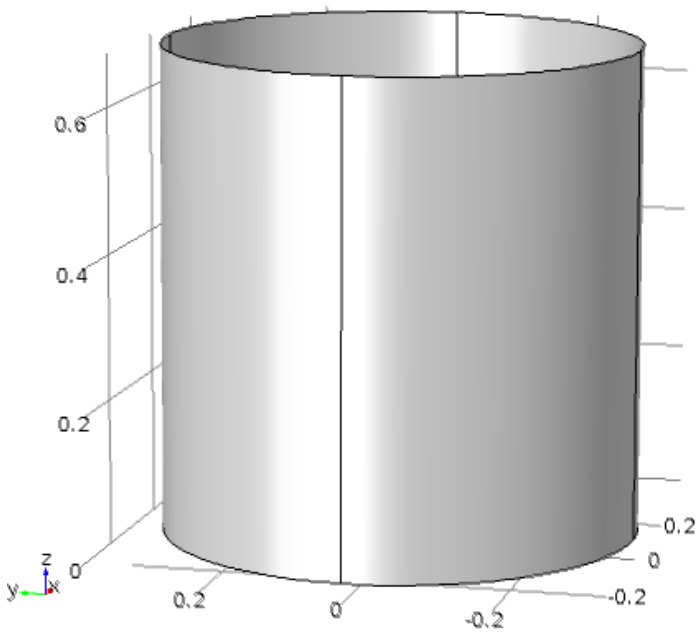

Figure 15 Geometry - Comsol

5.2.1 Post Processing

- *Film Thickness Plot*

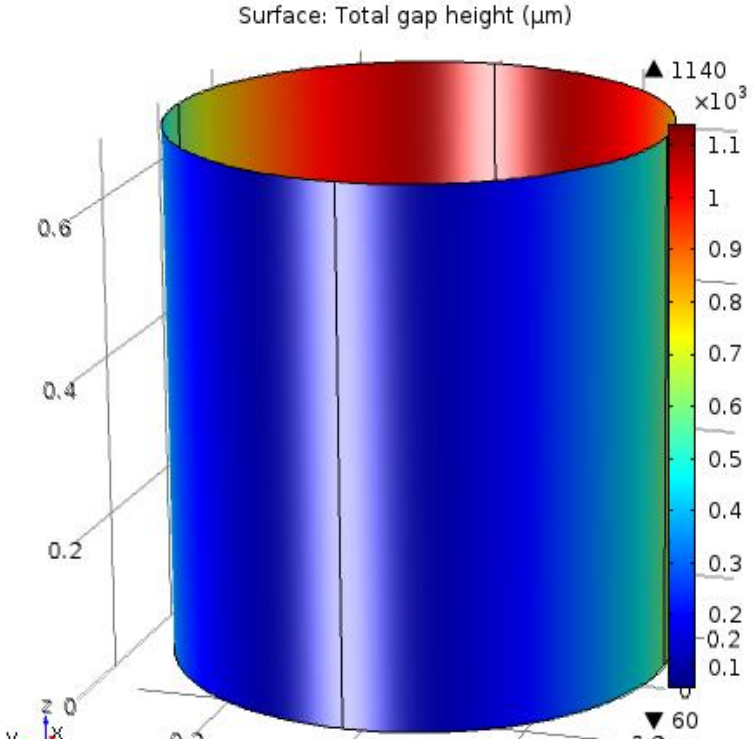

Figure 16 Film thickness plot

Therefore minimum film thickness (theoretical) is:

$$h_m = 81\mu m$$

And from Comsol plot, we obtained:

$$h_m = 60\mu m$$

- *Pressure Plot*

Pressure Plot is shown below with maximum pressure at the location of minimum film thickness and is nearly 10000 Pascal which is much lower than the yield strength of the material of bearing i.e. bronze.

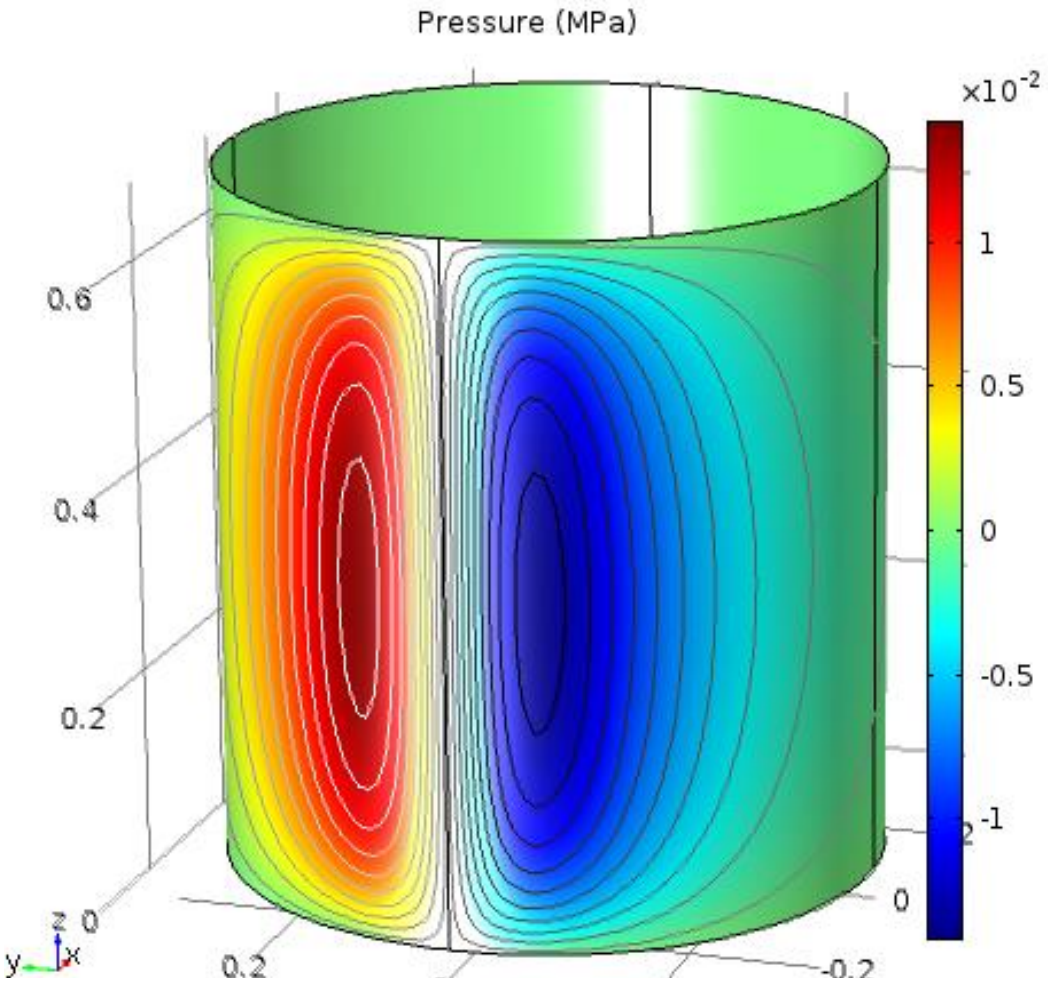

Figure 17 Pressure plot

- *Velocity Vectors*

Velocity vectors are shown below which show the rotation of journal

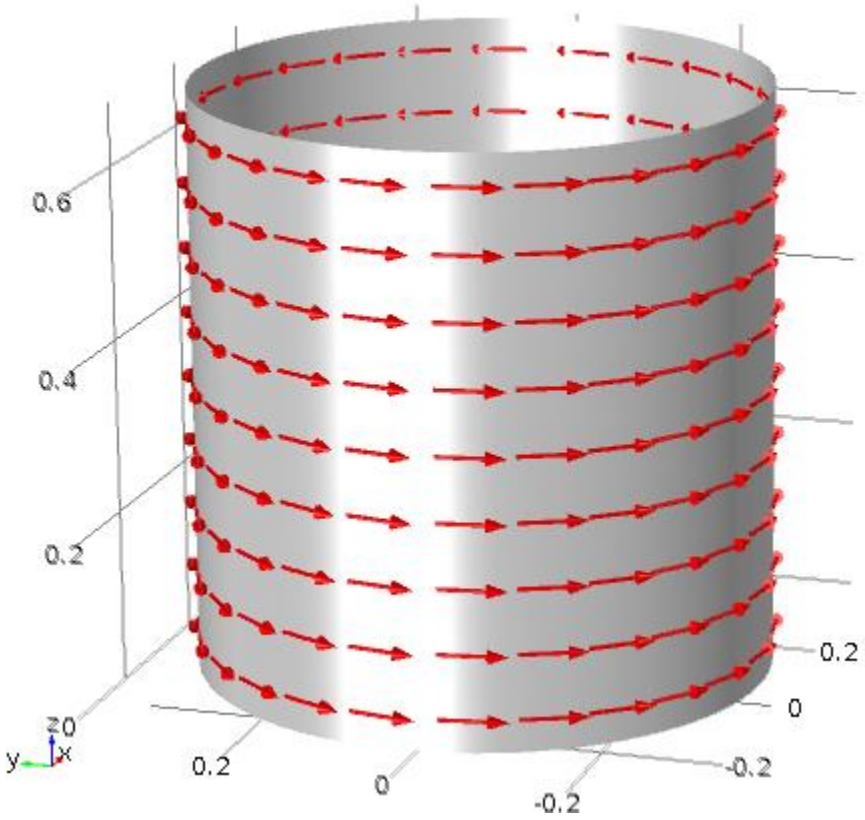

Figure 18 Velocity vectors

6 Heat Transfer Analysis

ANSYS Fluent was used to carry out a heat transfer analysis from the surface by the action of the coolant – water. The conditions as discussed in the initial chapters was maintained to gain realistic results. Furthermore a heat flux of 1400 W/m^2 was provided, which was the calculated heat flux being generated. Energy equation was turned on and k-epsilon model was used for turbulence of the flow.

The Solidworks model is as shown below, along with the fluid cavity portion.

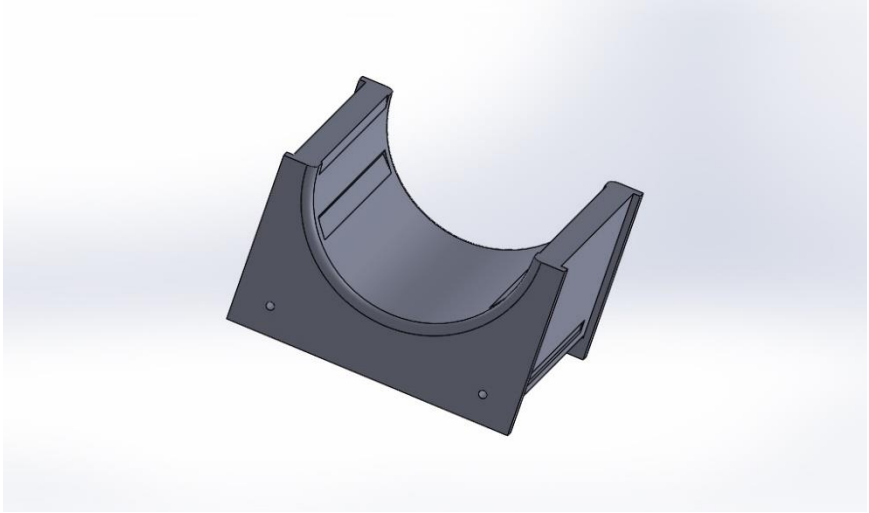

Figure 21 Solidworks model I

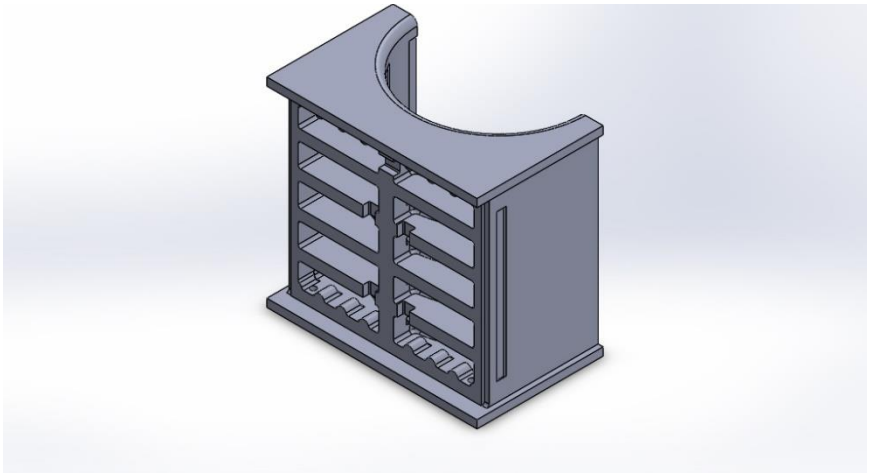

Figure 20 Solidworks model II

Figure 19 Fluid body in cavity

Since the bearing is symmetrical about the plane through the center of its arc, we do not need to simulate the entire bearing. In fact, each 'triangular' portion is a similar figure and the pattern is repetitive after three such portions. A good simulation practice would be to use a single repeat portion to save simulation time and power, causing minimal compromise on the results. The

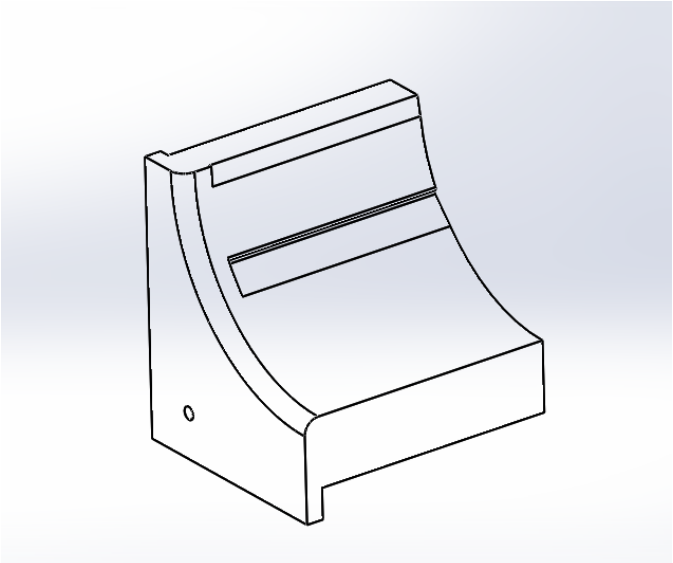

Figure 23 Sectioned geometry

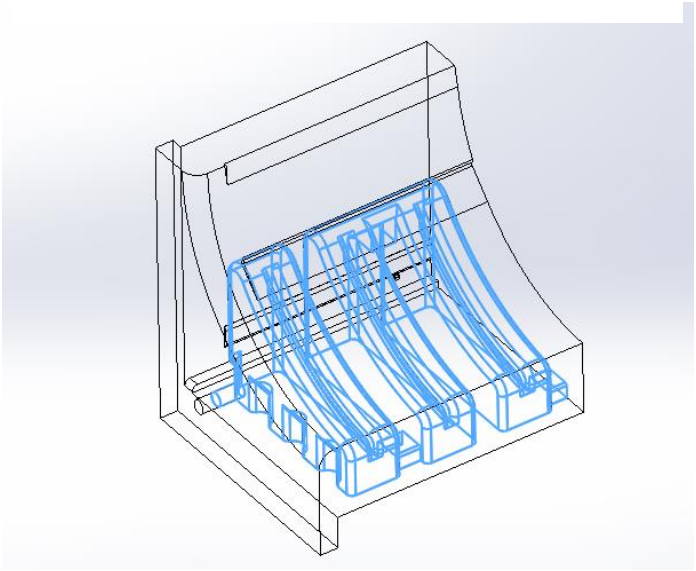

Figure 22 Sectioned geometry with cavity

portion used for all simulations is shown below.

6.1 Streamline Study

The first simulation carried out was intended to depict the results of the streamlines that form as the coolant water flows through the cavity. The results are as shown.

- *Velocity Streamline*

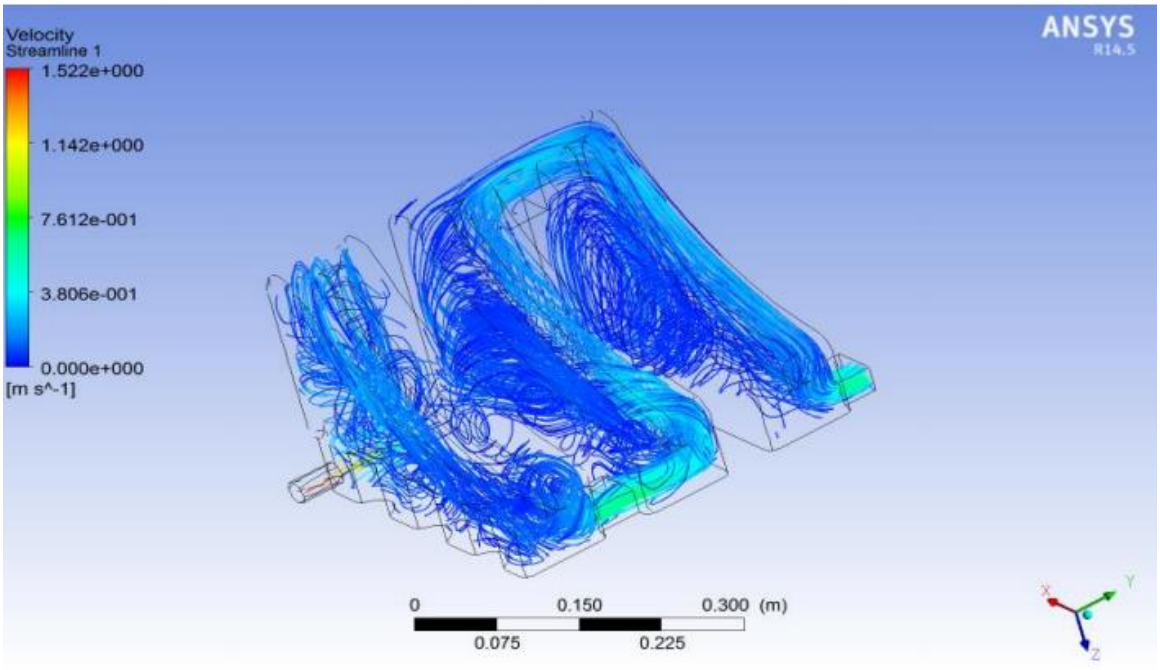

Figure 24 Velocity streamlines

The results show a lot of vortices being formed, which could potentially be a major hindrance in the flow of water and could be the cause of the failure.

- *Eddy Viscosity*

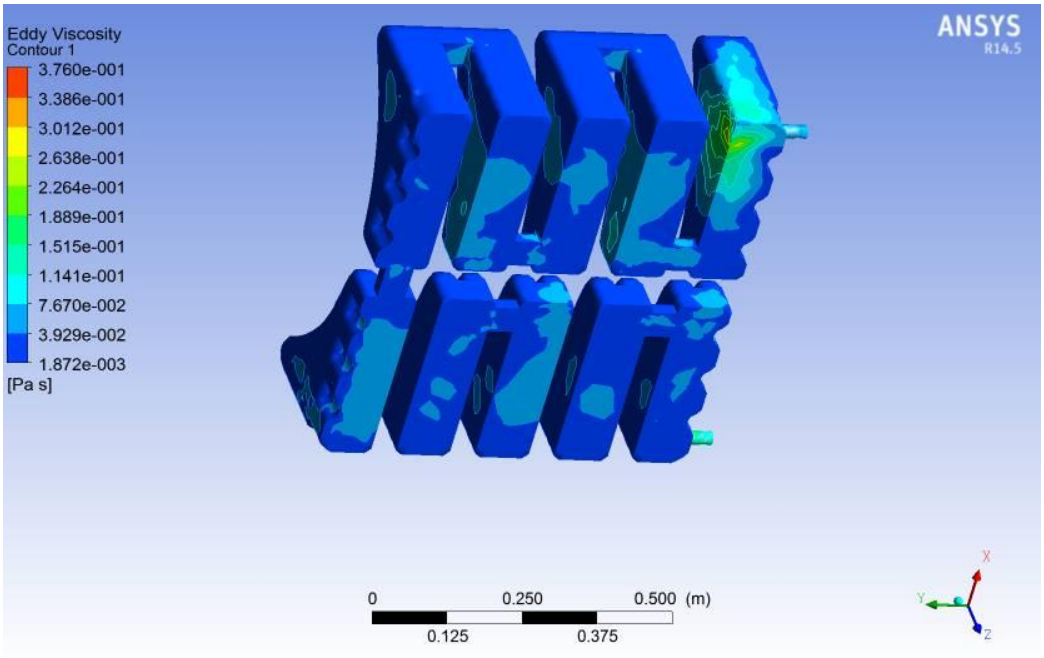

Figure 26 Eddy viscosity

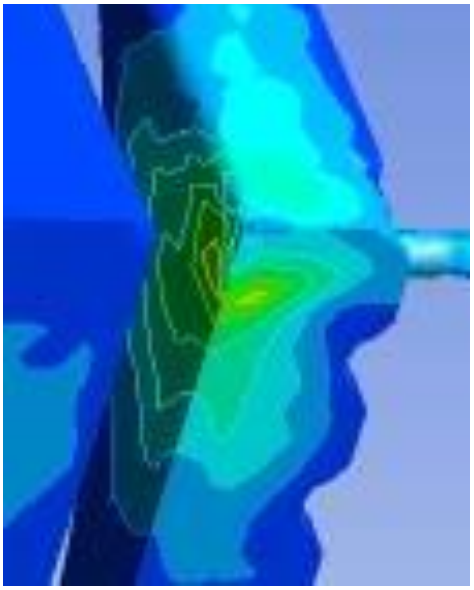

Figure 25 Zoomed in section of Fig 24

The results clearly show that the eddy viscosity are extremely high at the impact with the first wall.

This further proves difficulties in smooth fluid flow.

6.2 Bearing Temperature Study

The second simulation included interfacing of the fluid with the casing to find out the temperature contour formed on the surface of the bearing. The meshed body is as shown.

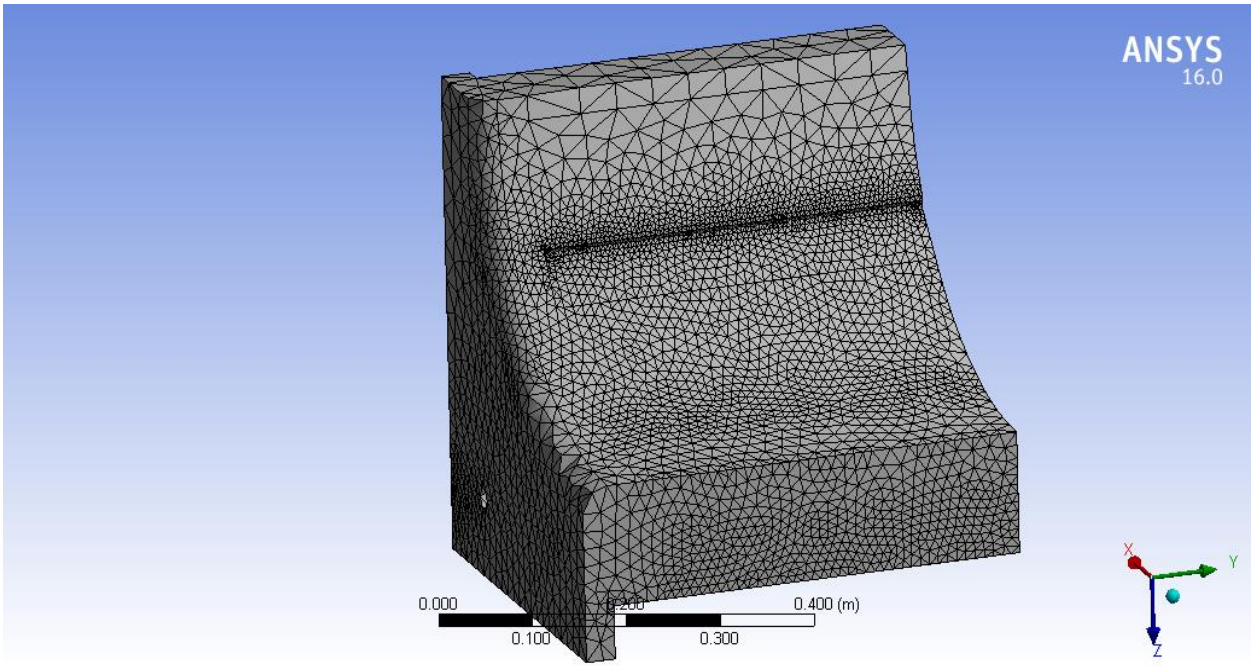

Figure 27 Meshed geometry

The results are as shown below.

- *Temperature Contour*

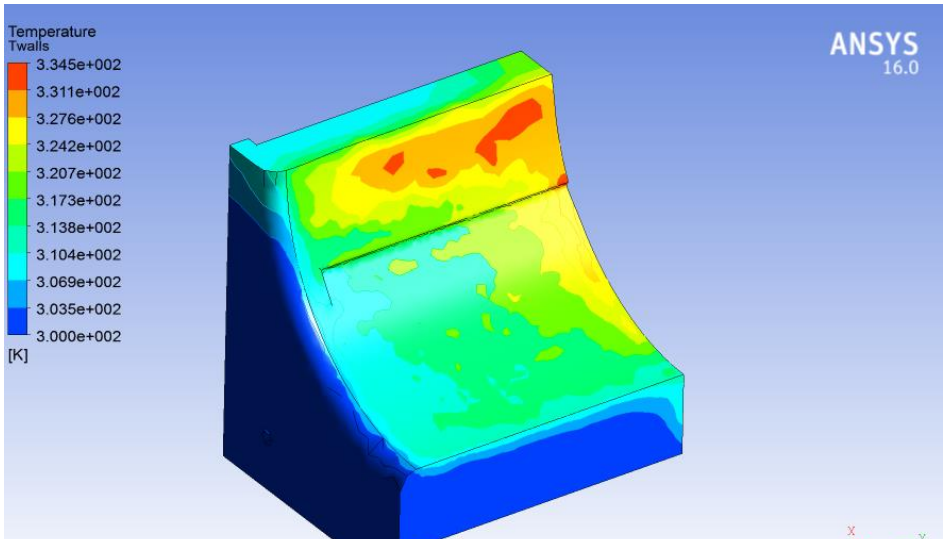

Figure 28 Temperature contour

- *Pressure Contour*

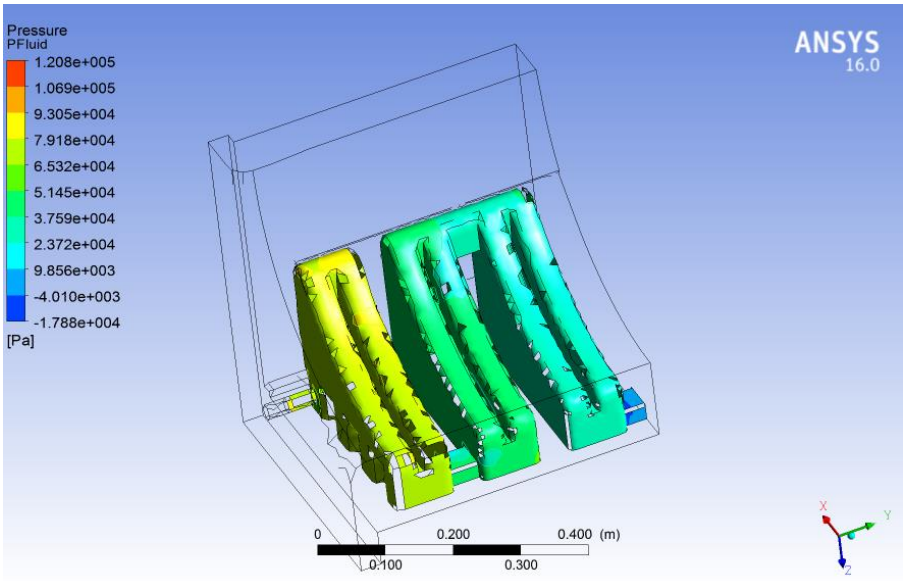

Figure 29 Pressure contour

- *Velocity Vector*

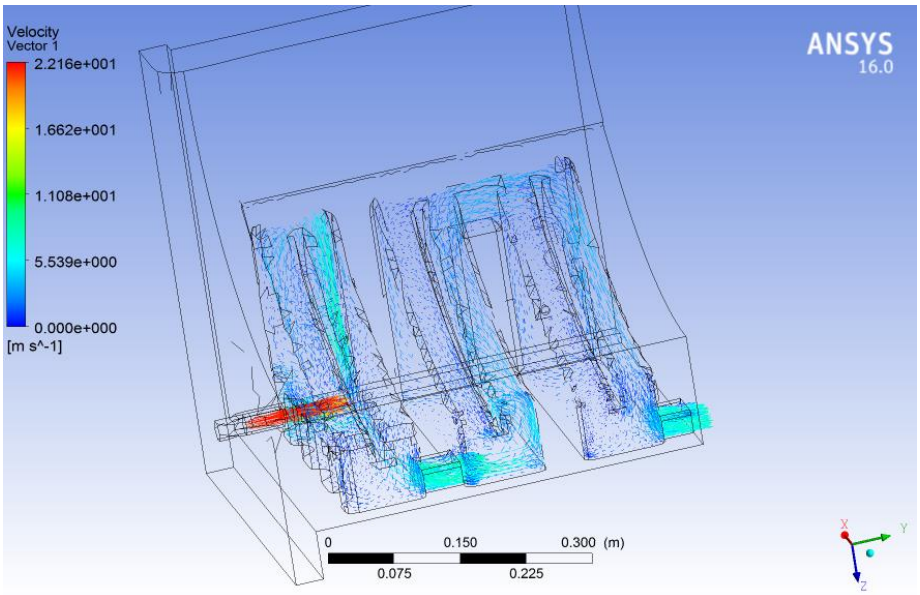

Figure 30 Velocity vectors

- *Velocity Streamline*

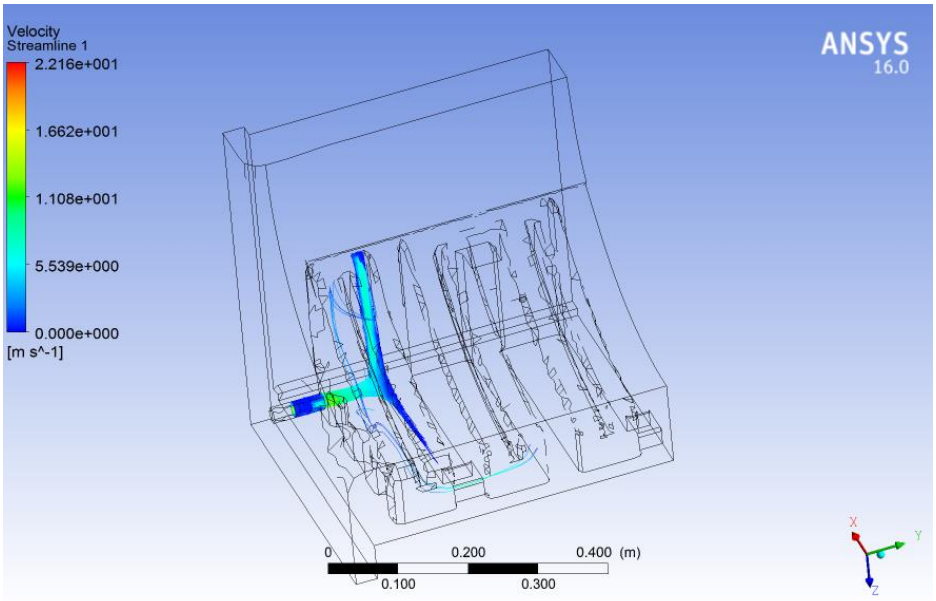

Figure 31 Velocity streamlines

- *Eddy Viscosity*

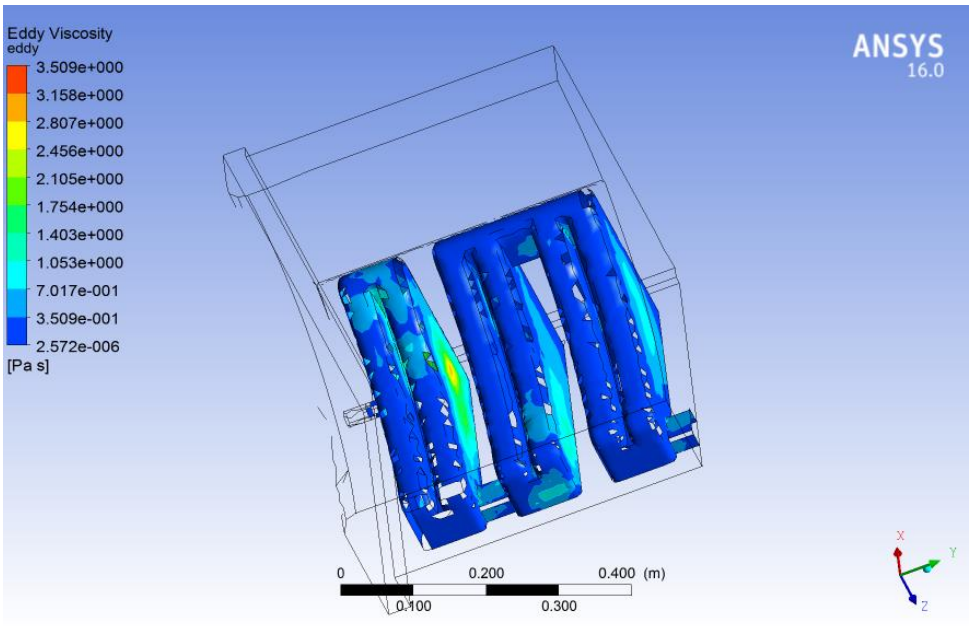

Figure 32 Eddy viscosity

6.2.1 Heat Transfer Calculations

Basic heat transfer calculations have revealed that heat generation due to friction is approximately 900 W. With the bearing surface area absorbing this heat being 0.676 m^2, the heat flux becomes close to 1400 W/m^2.

Using the specifications of the lubricant described earlier in the report, the maximum heat absorbed by it is merely 4.34 W. On the other hand, at a mass flow rate of water of 0.4 Kg/s and assuming a temperature rise of 4°C for water, we get a maximum heat removal potential of 10003.2 W from the coolant.

With the heat generated assumed to be entirely transferred from the top to the internal surface of the casing, i.e. throughout the thickness of the casing, the temperature of the bearing internal surface would be 40°C. At these conditions potential convective heat transfer to water is 1050 W.

To summarize this section, the theory suggests that the entire heat produced should be removed by the coolant at the conditions specified. However, simulations have revealed a temperature rise over the limit and is backed up by the actual case. Therefore, the results require further interpretation before a solution can be established.

7 Design Optimization

7.1 Interpretation of Results

The results of these simulations clearly reveal that the calculated minimum film thickness is very close to the value obtained from Comsol which implies that the film thickness is never zero, so the phenomenon of boundary lubrication is not taking place. The maximum pressure which we

obtained is nearly 15000 Pascal which is much lower than the yield strength of brass. The low pressure is due to very slow speed of journal. Hence it can be concluded that the failure is not occurring due to lubrication.

On the other hand, it can be safely assumed that the cause of the failure is heat related. Even though the coolant has enough capacity to remove the heat being generated, we have seen the temperatures exceeding the limit. A closer inspection of the model reveals the temperature goes high at the region where no cavity runs. In fact, the cavity only reaches up to the lubrication groove and never beyond it. Hence, the region above the groove does not have heat removed from it directly. This is shown in the figure below.

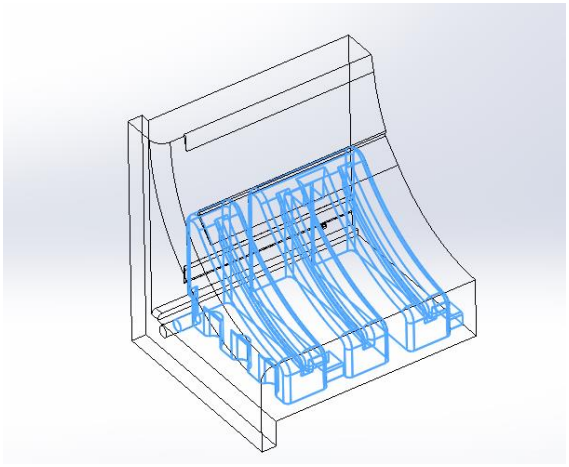

Figure 35 Geometry section with cavity

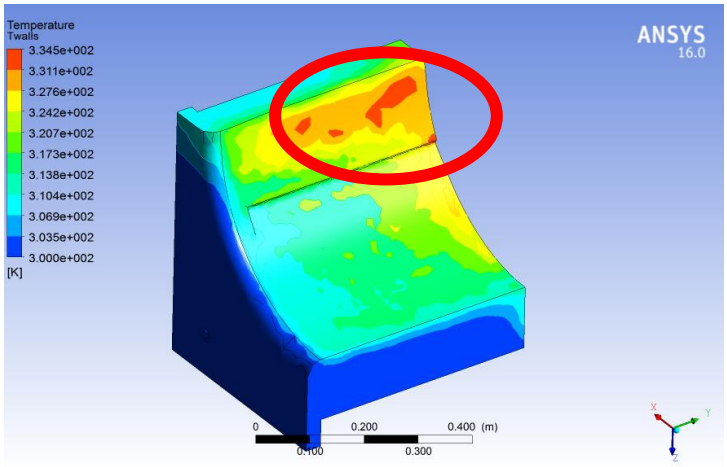

Figure 34 Temperature contours

Figure 33 Failed specimen III

Hence it can be concluded that the vortices and pressure drop across each section due to eddy viscosities is not the cause of the failure. The overheating of the component is not attributed to insufficient heat removal but rather to inefficient heat removal, which shall be worked upon later in the project.

7.2 Redesigning

Now that it has been established that the region under which no cavity reaches is the one which gets overheated, redesigning involved extending the cavity. The side wall was extruded outwards to give a plane face to ensure the strength of the component is no compromised by extension of the cavity. Also, in an attempt to make the cavity as large as possible, it has been extended all the way up until a margin of 10% of the height from the top, as shown in the figures below.

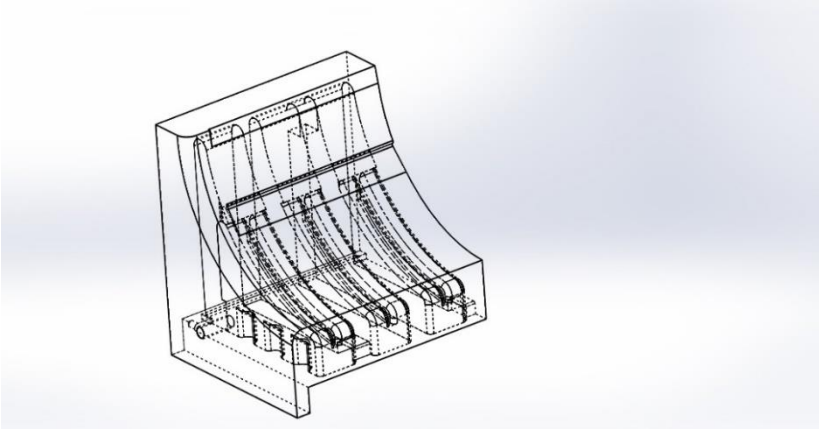

Figure 36 Redesigned model I

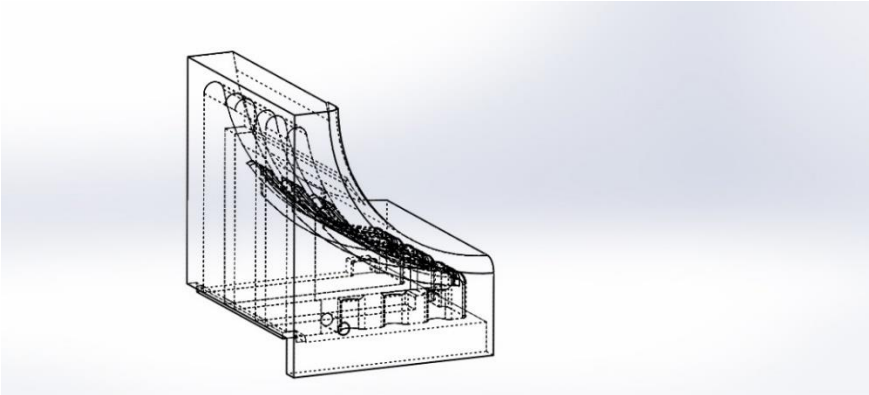

Figure 37 Redesigned model II

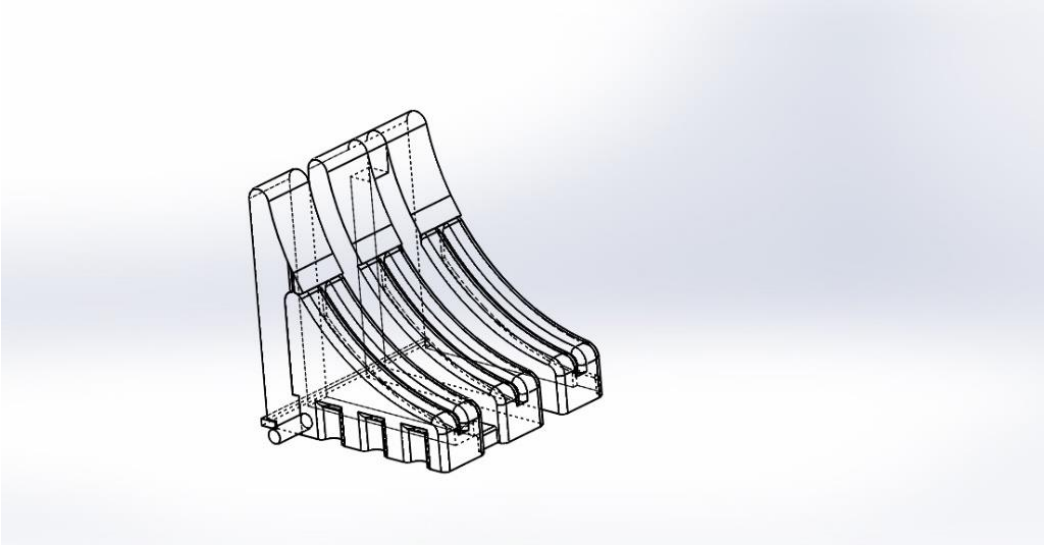

Figure 38 Fluid body in redesigned cavity

7.3 Design Evaluation

The new design has been tested by simulating it on ANSYS Fluent under the same parameters. The results gained were significantly better, with no region getting overheated. In fact, the variation in temperatures over the surface was very low and a near uniform temperature was achieved. Moreover, the pressure losses were reduced as a larger breathing space was provided to the coolant and, hence, the flow experienced less vortices. The results are show in figures below.

- *Temperature Contour (Casing Surface)*

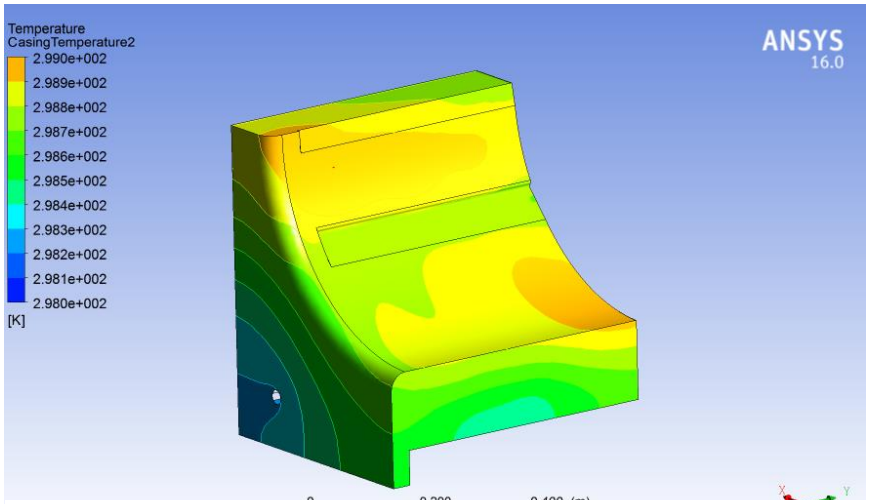

Figure 39 Temperature contours (casing surface)

- *Temperature Contour (Liquid Surface)*

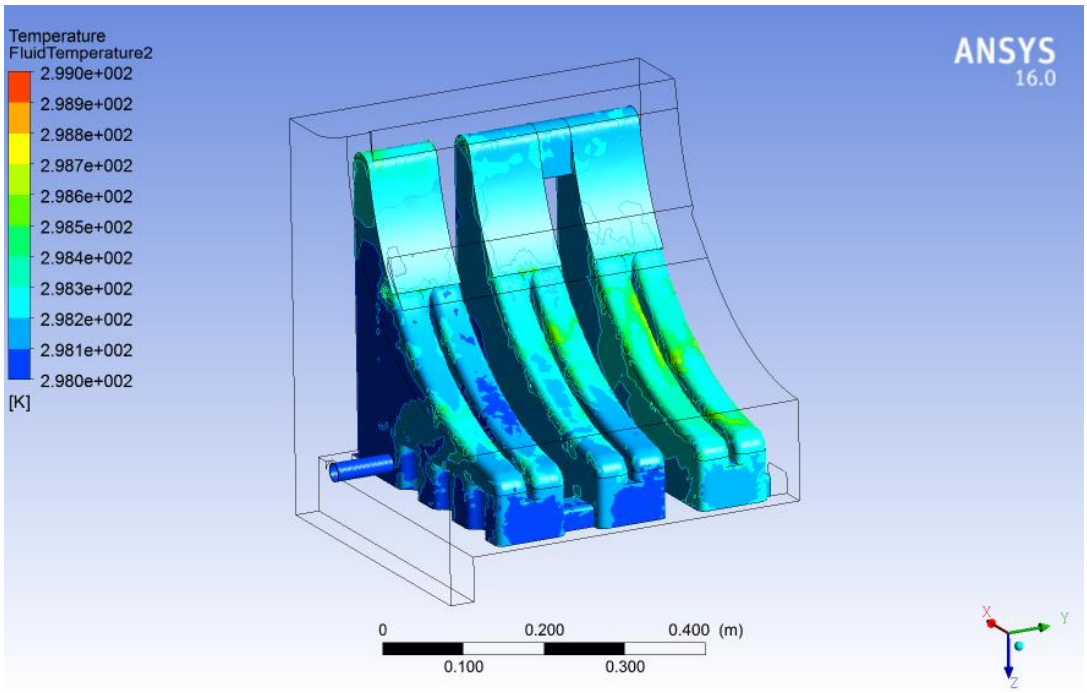

Figure 40 Temperature contours (liquid surface)

- *Velocity Streamlines*

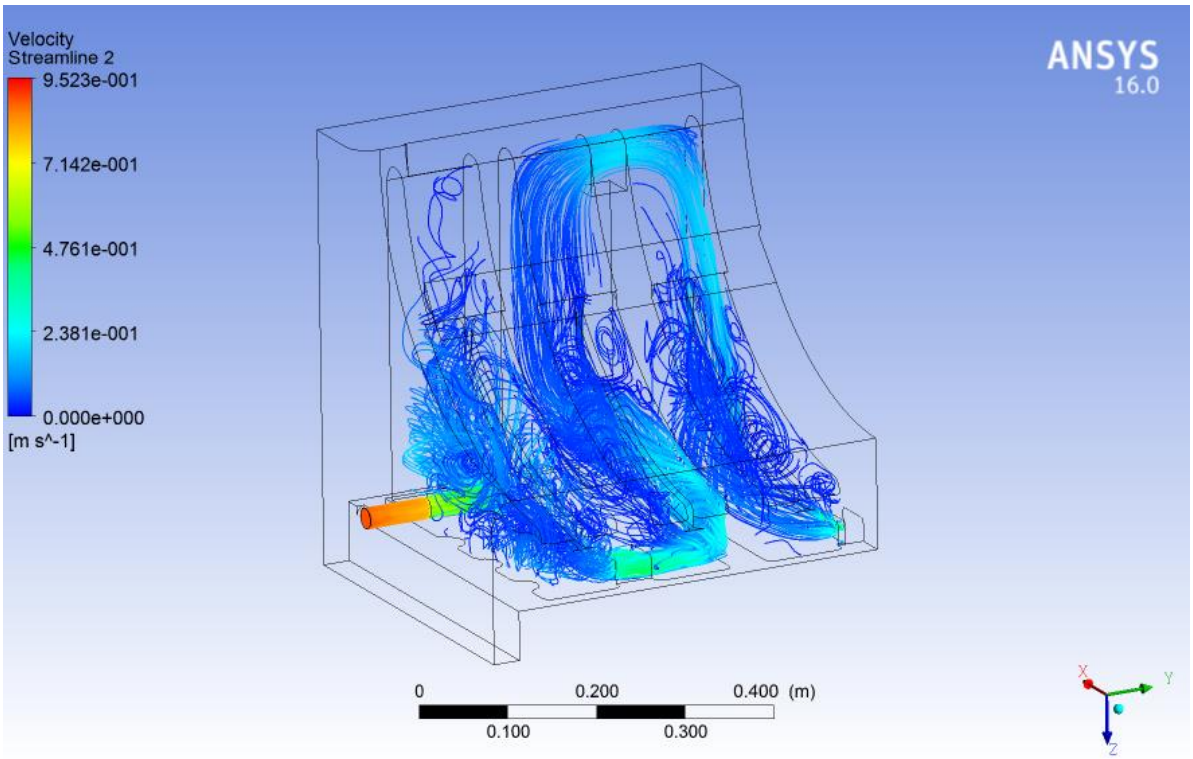

Figure 41 Velocity streamlines

- *Velocity Vectors*

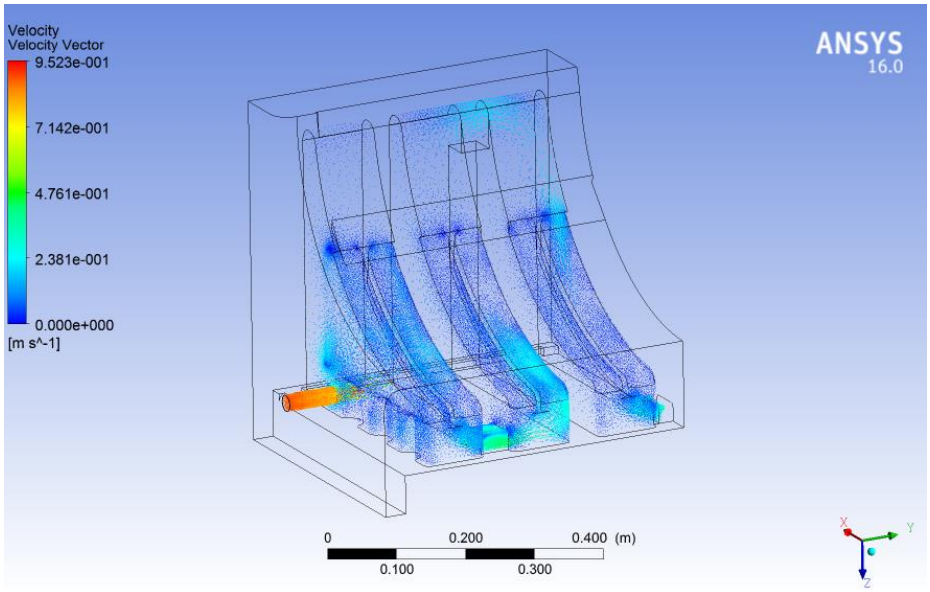

Figure 42 Velocity vectors

7.4 Manufacturing

The portion of the bearing that has been used for simulation has been considered for manufacturing purposes as well. We have manufactured (by sand casting) both designs and a comparative study is done. However, the dimensions have been scaled down by a factor of 0.5 to limit the costs. Also, aluminum has been used instead of bronze. This is due to the fact that aluminum is easily available and, again, cost effective as compared to bronze. These factors are no expected to effect the outcomes since the model prototype is analogous to the original component in terms of design and operation. Since the purpose of this model is to carry out a comparison of the heat removal system of the original and redesigned bearing, it is expected to do so, given both of them are run under the same conditions.

It should be noted that due to the unavailability of test rig along with the limited scope of this project a running shaft or an alternative heat source could not be used. However, rather than flow cold water to remove the heat, hot water will be pumped through the cavity and the rise in the top surface is measured. The process, although reversed, fulfills our purposes of comparing heat transfer – one way or the other.

Test run clearly shows that the redesigned bearing has a better heat transfer.

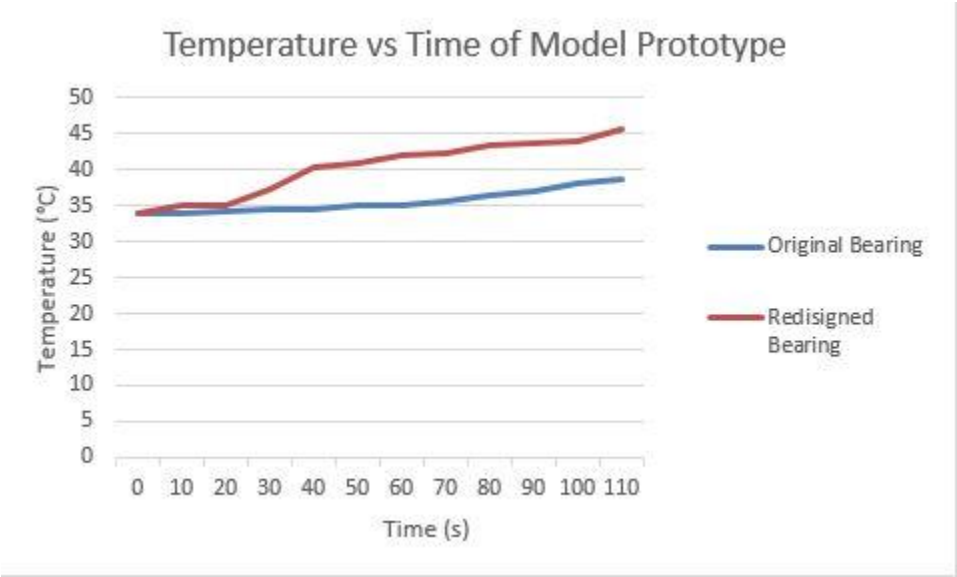

Figure 43 Temperature vs Time of prototype models

The manufactured prototype is shown in the figures below.

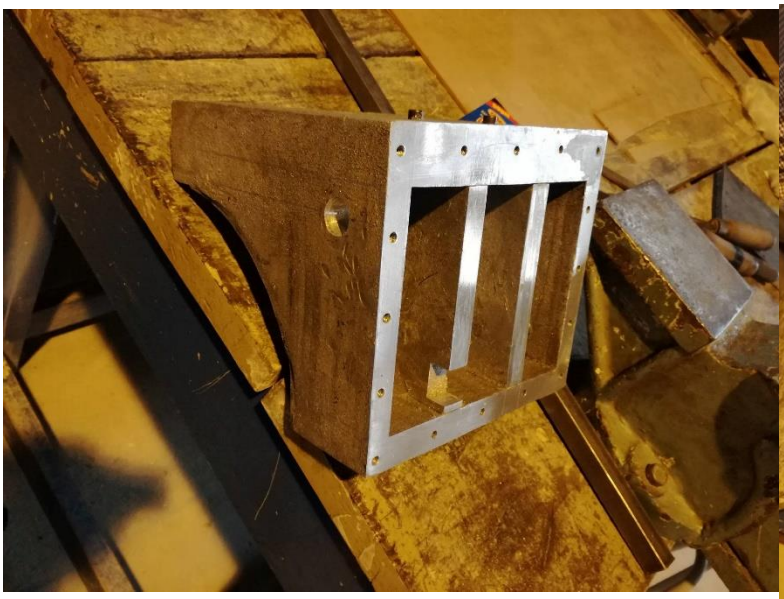

Figure 44 Prototype I

Figure 45 Prototype II

8 Conclusion

To conclude and summarize the project, the failure analysis study of Qadri Group's mill top journal bearing, using FMEA, pointed out the cause to be in the cooling system. The cooling system has been successfully modified accordingly to cater for the thermal dissipation problem. The maximum temperature in the bearing has been reduced from 335 K to 300 K, resulting in a 10% increase in the effectiveness of the cooling system.

Additionally, the new design has reduced the weight of the bearing from approximately 122 Kg to 95 Kg as a result of an increased volume of cavity from 0.05 m^3 to 0.06 m^3; thereby reducing material costs by roughly 22%. The fishbone diagram below summarizes the failure modes.

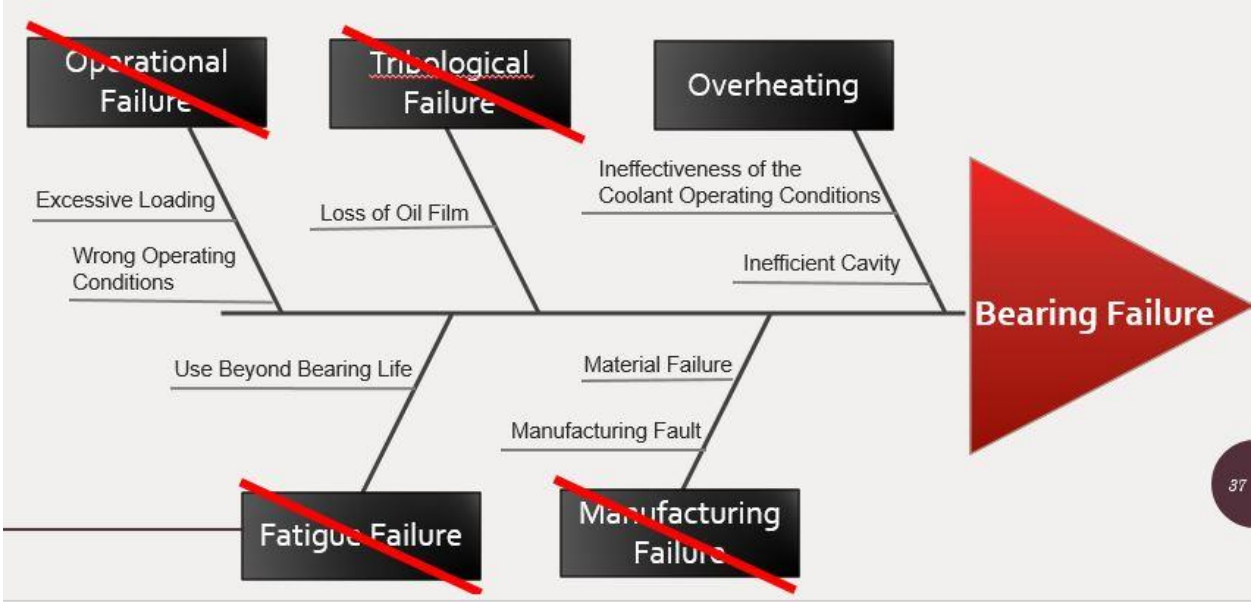

Figure 46 Fishbone diagram

Moreover, a bearing Failure Mode Effects Analysis standard methodology has been devised using analytical and numerical methods which can be implemented to any component failure diagnostics with suitable modifications.

9 References

[1] S. M. Muzakkir, "Tribological Failure Analysis of Journal Bearings Used in Sugra Mills," *Engineering Failure Analysis*, vol. 18, no. 8, p. 2093–2103, 2011.

[2] "Alpha SMR Range - Castrol MSDS Search," 20 October 2015. [Online]. Available: http://msdspds.castrol.com/bpglis/FusionPDS.nsf/Files/97C29D4896A7567480257EE40026A528/$File/BPXE-A3RBGV.pdf. [Accessed 17 February 2017].

[3] M. E. Leader, "Undertranding Journal Bearings," [Online]. Available: http://edge.rit.edu/edge/P14453/public/Research/2-_LEADER_-_Understanding_Journal_Bearings.pdf. [Accessed 16 January 2017].

[4] S. Singhal, "Sleeve Bearing Design for Slow Speed Applications in Cement Plant," in *IEEE*, Miami, FL, USA, USA, 2008.

[5] D. J. Hargreaves, "The Lubrication of Mill Brasses," in *Austrailian Society of Sugar Cane Technologists*, 1984.

[6] J. Layer, "Failures of Sliding Bearings," in *ASM Handbook Vol 11 - Failure Analysis and Prevention*, ASM Handbook Committee, 2002, pp. 2344-2360.

[7] M. S. M. H. H. G. D. T. Lijesh K. P., "Control on wear of journal bearing operating in mixed lubrication regime using grooving arrangements," *Industrial Lubrication and Tribology*, vol. 68, no. 4, pp. 458-465, 2015.

[8] A. W. B. Gwidon W. Stachowiak, Engineering Tribology - Third Edition, Butterworth-Heinemann, 2005.

[9] [Online]. Available: http://henrysbench.capnfatz.com/henrys-bench/arduino-temperature-measurements/max6675-temp-module-arduino-manual-and-tutorial/. [Accessed 24 May 2017].

[10] A. F. Incorporated, *Standard Properties of Typical Brass, Bronze and Aluminum Alloys*, Illinois : AluBra Foundary Incorporated, 2016.

[11] [Online]. Available: http://www.bmpcoe.org/library/books/mil-hdbk-338b/a211.html. [Accessed 24 May 2017].

[12] [Online]. Available: http://www.syque.com/quality_tools/toolbook/FTA/how.htm. [Accessed 13 May 2017].

10 Appendix 1 – Design Evaluation Calculations

10.1 Surface Speed (FPM)

$$FPM = RPM\left(\frac{\pi D}{12}\right) [3]$$

$$= (5)(\pi)\left(\frac{25.98}{12}\right) = 34.01$$

Where D = Diameter (in)

10.2 Specific Steady Load

$$P = \frac{W}{LD} [3]$$

$$= \frac{40000}{(32.28)(25.89)} = 47.86\ PSI$$

Where,

W = Load (lb)

L = Axial Length (in)

11 Appendix 2 – Simulation Verification Calculations

11.1 Lubrication Calculations

11.1.1 Theoretical Film Thickness

$$h_m = \frac{2c(1-\varepsilon^2)}{2+\varepsilon^2}$$

Where,

$c = clearnace = 0.6mm$

$\varepsilon = eccentircity\ ratio = 0.9$

11.2 Heat Transfer Calculations

11.2.1 Heat Generation

Friction power, $H_f = T\omega = T\pi n = (\frac{\pi^2 \eta n R^4}{h})(\pi n)$ [8]

$$(\frac{\pi^2 X 3.04 X 10^{-3} X 5 X 0.66^4}{1 X 10^{-3}})(\pi X 5)$$

= 894.4 W

Where,

T = Torque needed to rotate the bearing (Nm)

ω = Bearing angular velocity (rad/s)

n = Speed of the bearing (rev/s)

η = Dynamic viscosity (Pas)

R = Radius (m)

h = film thickness (m)

11.2.2 Heat Flux

$$= \frac{H_f}{A} = \frac{894.4}{0.676}$$

= 1323 W/m^2

≈1400 W/m^2

Where,

A = Surface area of bearing with shaft contact (m^2)

11.2.3 Heat Absorbed by the Oil

$$H = \dot{Q}\rho\sigma\Delta T \text{ [8]}$$

$$\left(1.23\ X\ 10^{-4}\right)(0.949)(1860)(20) = 4.34\ W$$

Where,

$\dot{Q}$ = volume flow rate (m^3/s)

ρ = density (kg/m^3)

σ = specific heat capacity (J/Kg.K)

11.2.4 Maximum Heat Removal Capacity of Water

$$\dot{Q} = \dot{m}c\Delta T$$

$$= (0.4)(4180)(4) = 1003.2\ W$$

For an assumed temperature change of 4°C.

Where,

$\dot{m}$ = mass flow rate (Kg/s)

11.2.5 Conductive Heat transfer to the Lower Surface

$$\dot{Q} = kA\left(\frac{\Delta T}{\Delta x}\right)$$

$$\Delta T = \frac{870\ X\ 75\ X\ 10^{-3}}{100\ X\ 0.68} = 4.66$$

$$T_2 = 40\ °C$$

Assuming that the entire heat is transferred to the lower surface.

Where,

K = coefficient of conductivity = 100 (W/m.C)

T_2 = Temperature at the inner surface of the bearing (°C)

11.2.6 Convective Heat Transfer to Water

$$\dot{Q} = hA\Delta T = (500)(0.14)(15) = 1050W$$

Where h = coefficient of convection = 500-1000 (W/m^2.°C) for forced convection in a tube

12 Appendix 3 – Data Acquisition

12.1 Arduino Code [9]

```
#include "max6675.h"

int ktcSO = 8;

int ktcCS = 9;

int ktcCLK = 10;


MAX6675 ktc(ktcCLK, ktcCS, ktcSO);


void setup() {
```

```
  Serial.begin(9600);
  // give the MAX a little time to settle
  delay(500);
}

void loop() {
  // basic readout test

   Serial.print("Deg C = ");
   Serial.print(ktc.readCelsius());
   Serial.print("\t Deg F = ");
   Serial.println(ktc.readFahrenheit());

   delay(200);
}
```